Journal of Medicinal Chemistry

Article

Design, Synthesis and Antitumor Evaluation of Novel Histone Deacetylase (HDAC) Inhibitors Equipped with Phenylsulfonylfuroxan Module as Nitric Oxide (NO) Donor

Wenwen Duan, Jin Li, Elizabeth S. Inks, C. James Chou, Yuping Jia, Xiaojing Chu, Xiaoyang Li, Wenfang Xu, and Yingjie Zhang

J. Med. Chem., **Just Accepted Manuscript** • DOI: 10.1021/acs.jmedchem.5b00317 • Publication Date (Web): 23 Apr 2015

Design, Synthesis and Antitumor Evaluation of Novel Histone Deacetylase (HDAC) Inhibitors Equipped with Phenylsulfonylfuroxan Module as Nitric Oxide (NO) Donor

Wenwen Duan,[†] Jin Li,[†] Elizabeth S. Inks,[‡] C. James Chou,[‡] Yuping Jia,[§] Xiaojing Chu,[‖] Xiaoyang Li,[†] Wenfang Xu [†] and Yingjie Zhang [†*]*

[†]Departments of Medicinal Chemistry, School of Pharmacy, Shandong University, Ji'nan, Shandong, 250012, People's Republic of China

[‡]Department of Drug Discovery and Biomedical Sciences, South Carolina College of Pharmacy, Medical University of South Carolina, Charleston, South Carolina 29425, United States

[§]Shandong Academy of pharmaceutical Sciences, Ji'nan, Shandong, 250101, People's Republic of China

[‖]Weifang Bochuang International Biological Medicinal Institute, Weifang, Shandong, 261061 , People's Republic of China

ABSTRACT: Based on the strategy of "multifunctional drugs," a novel series of phenylsulfonylfuroxan-based hydroxamates with histone deacetylase (HDAC) inhibitory and nitric oxide (NO) donating activities were designed, synthesized, and evaluated. The most potent NO donor-HDAC inhibitor (HDACI) hybrid **5c** exhibited much more potent in vitro

antiproliferative activity against human erythroleukemia (HEL) cell line than the approved drug SAHA (Vorinostat), and its antiproliferative activity was diminished by the NO scavenger hemoglobin in a dose-dependent manner. Further mechanism studies revealed that **5c** strongly induced cellular apoptosis and G1 phase arrest in HEL cells. Animal experiment identified **5c** as an orally active agent with potent antitumor activity in a HEL cell xenograft model. Interestingly, although compound **5c** was remarkably HDAC6 selective in the molecular level, it exhibited pan-HDAC inhibition in the western blot assay likely due to NO release causing class I HDACs inhibition in the cellular level.

■ Introduction

The important role of histone deacetylation in gene expression and regulation, especially in the pathogenesis of cancer has been reported by numerous researchers since the 1960s. Histone deacetylases (HDACs) are a family of enzymes, which catalyze acetyl-group removal from the lysine residue in the histone tails and lead to a transcriptionally repressed chromatin state.[1, 2] Abnormal HDAC activity has been found to be associated with the aberrant gene expression and the development of several kinds of cancer and other human ailments.[3, 4] Accordingly, HDAC inhibition restores normal gene expression profile resulting in cancer cell cycle arrest, cell differentiation, and apoptosis. Thus, HDAC inhibitors (HDACIs, Figure 1),[3, 5] which block abnormal HDAC deacetylation have been recently developed and validated as potential anticancer agents, such as hydroxamic acids, short chain fatty acids, cyclic tetrapeptide, and benzamides. Among these HDACIs, hydroxamic acids have been the most well-known ones with

SAHA (**6**, Figure 1) , PXD-101(**7**, Figure 1) and LBH-589(**8**, Figure 1) approved by the US Food and Drug Administration (FDA) in October 2006, July 2014 and February 2015 for the cancers[6, 7] respectively in the clinic. Many other hydroxamate compounds are in the clinical trials, such as SB-939 (**9**, phase II, Figure 1), and 4SC-201(**10**, phase II, Figure 1).[3, 8]

(Figure 1 should be listed here)

Cellular Nitric Oxide (NO), described in 1980 by Forchgott, participates in the vascular regulation, nerve transmission delivery, inflammation, and immune response process as an important massager molecule in organism.[9, 10] NO can also inhibit tumor cells proliferation,[11] angiogenesis, metastasis,[12] and accelerate tumor cell apoptosis.[13] In addition to the inducible nitric oxide synthase (iNOS), which can produce a heavy dose of cellular NO by stimulating factors such as cytokins, chemical NO donor is also an effective way to generate a high concentration of cellular NO. It was reported that glyceryl trinitrate (GTN) can inhibit the proliferation of tumor cells P388 and L-1210 in vitro and in vivo.[14] Sodium Nitroprusside (SNP) was reported to exhibit potential cytotoxicity to the leukemia cells of ML, AML, and CMMOL.[15] Oxadiazole (**22**, Figure2) was found in 2008 through a high throughput screen to be an important and potential NO donor, which could produce high levels of NO in vitro and inhibit the growth of tumor in vivo.[16, 17] Phenylsulfonylfuroxan (**23**, Figure 2), aclassical type of oxadiazole, is stable in acidic and basic conditions, and its mechanism of NO release in vivo was determined to be through its reaction with mercapto-compound such as cysteine as described by Feelisch in 1992.[18] It can also release NO to produce activity in variety of tissues and organs through a

non-enzymatic pathway. Compounds like phenylsulfonylfuroxan coupled with oleanolic acid, farnesylthiosalicylic acid, or anilinopyrimidine have displayed synergistic anti-tumor activity.[19, 20, 21, 22]

(Figure 2 should be listed here)

Over the past decades, an increasing body of research reported that covalent modifications, such as S-nitrosylaion or tyrosine-nitration of proteins by NO can dramatically influenced their cellular functions. Interestingly, many HDAC family members have also been found to be direct or indirect targets of NO,[23] and several reports have illustrated that NO-dependent regulation of HDAC functions.[24] HDAC family consists of eighteen isoforms[2, 3] belonging to four structurally and functionally different phylogenetic classes: class I (HDAC 1, 2, 3, and HDAC 8), class II (class IIa: HDAC 4, HDAC 5, HDAC 7, HDAC 9; class IIb: HDAC 6 and HDAC 10) and class IV (HDAC 11) are called "classical HDACs" and are Zn^{2+} dependent proteases. While the class III (SIRT 1~7) are NAD^{+} dependent. The enzymatic activity of class I enzyme HDAC 2 and HDAC 8 have been reported to be directly inhibited by NO-dependent S-nitrosylation.[24, 25] S-nitrosylation of HDAC2 induces its release from chromatin.[26] The nuclear shuttling of class IIa HDAC is also induced by NO through sGC-cGMP pathway.[23] Furthermore, NO have been shown to allow crosstalk between class III and class I HDACs.[27] In fact, some studies have shown that HDACI and NO are synergistic in cardiac hypertrophy[28] and wound healing.[29, 30]

"Multifunctional drugs" through the hybridization strategy is a well-developed approach in

drug design process. It involves the combination of two complementary or synergistic pharmacophores directly or via a spacer in order to act on different targets to improve the activity. Recently, a hybrid (NO-MS275, **25**, Figure 3) of NO donor and HDACI MS275 (**24**, Figure 3) was reported to promote myogenic differentiation in a more efficient manner than the 1:1 mixture of the two components,[33] however no antitumor activity of this compound was reported. Based on the above mentioned analysis and the "multifunctional drugs" theory, the goal of this study is to develop novel HDACI containing the NO donor motif (Figure 4) that exhibits addictive antitumor activity via HDAC inhibition and NO release.

(Figure 3 should be listed here)

(Figure 4 should be listed here)

■ Result and discussion

Chemistry

Based on HDACI pharmacophore exemplified by SAHA (Figure 3), a series of novel target compounds containing phenylsulfonylfuroxan as NO donating module were designed and synthesized. The target compounds **5a**-**5o** were synthesized from (phenylthio)acetic acid (purchased from Adamas-beta, China) as shown in Scheme 1. The compounds **2** and **3** were synthesized following the method of Zhang's.[22] One-pot reaction of (phenylthio)acetic acid by oxidization with 30% H_2O_2 aqueous solution resulted in compound **1**, which was refluxed after

adding fuming HNO_3 without purification to get compound **2**. After nucleophilic substitution by several corresponding linkers with two hydroxyl groups, we synthesized various monophenylsulfonylfuroxans (compounds **3a-3n)**, which were oxidized under *Jones* agent to get compounds **4a-4n**. The target compounds **5a-5n** were obtained from **4a-4n** under the conditions of isobutyl chlorocarbonate, triethylamine, and hydroxylamine hydrochloride. Compound **3j** was also oxidized by PCC to make compound **6**, which was reacted with propandioic accid to get compound **7**, and then transformed to the target hydroxamate **5o**.

(**Scheme 1** should be listed here)

Biological Results

Inhibiton of Hela Cell Extracts by the Target Compounds.

Based on the fact that all zinc ion dependent HDACs were highly conserved in their active sites, all target compounds were evaluated for their in *vitro* HDACs inhibitory activities using Hela cell extracts (containing primarily HDAC1 and HDAC2) as enzyme source and SAHA as positive control. The result listed in Table 1 revealed that the IC_{50} values of the compounds **5a** (0.047 μM), **5c** (0.038 μM), **5d** (0.054 μM), **5e** (0.063 μM) and **5j** (0.047 μM) were significantly lower than that of SAHA. This result revealed that the compounds containing the saturated fatty linker without any branched chains were more potent compounds than other linkers. When the linker was substituted with aromatic ring such as benzene, the IC_{50} values of those without substitutes were lower than analogs containing substitutes, and the hydroximic acid group was

best be located in the para-position to the phenylsulfonyllfuroxan. Generally, compounds containing saturated fatty linkers without any branched chains exhibited much more potency in HDAC inhibitory activities and the optimal length of the linker should be six to eight carbons. Our results also showed that compounds **2** and **3c** were not active against Hela cell nuclear extract, validating the crucial role of hydroxamate group in HDAC inhibition.

(**Table 1** should be listed here)

In Vitro Antiproliferative Assay.

Antiproliferative activities of target compounds **5a**-**5o** and **3c**, **2**, SAHA with **2** (1:1) were tested against HEL (human erythrocyte leukemia cell), HCT-116 (human colorectal carcinoma cell), Hela (human cervical carcinoma cell), U937 (Human Histiocytic leukemia cell line), 3-AO (human oophoroma cell), MDA (human breast cancer cell), ES-2 (Ovarian clear cell carcinoma cell), KG1 (human leukemia cell) cell lines by MTT (3-(4,5-dimethylthiazol-2-yl)-2,5-diphenyltetrazolium bromide) reduction assay, using SAHA as the positive control (Table 2). From the result listed in Table 2, it was found that the inhibitory activity against tumor cell growth of most of these compounds were better than the clinically approved drug SAHA, especially **5a**, **5b**, **5c** and **5j**, which exhibited higher HDAC enzyme inhibitory potency and with improved antiproliferative ability against cancerous cells. It should be noted that NO donors **2** and **3c** were also effective at againsting HEL cells proliferation and combination of SAHA and NO donor **2** with mole ratio of 1:1 exhibited dramatic additive effect.

In addition, cytotoxicity of **5c** against normal primary HUVEC (human umbilical vein endothelial cells) was tested in our lab, and the IC_{50} value was 27.1 μM, which revealed our compounds' selectivity over non-transformed cells when compared to tumor cells. Encouraged by these results, compound **5c** with the highest Hela nuclear extracts inhibitory potency and the best antiproliferative activity, was progressed to further in vitro evaluation using the most sensitive HEL cell line as cellular models.

(**Table 2** should be listed here)

NO Generation Measurement.

Regarding the effect of NO generation, the levels of NO generated by the tested compounds in vitro were detected. HEL cells were respectively exposed to 100 μM of **5a**, **5b**, **5c**, **5j**, **2**, and SAHA in the same incubation time (3 hours or 5 hours). The levels of NO released in the cell lysates were determined using a Griess assay. In Figure 5 we found that the compounds we designed and synthesized could release NO effectively, in contrast, SAHA hardly released any NO in HEL. Compound **5c**, which exhibited the most potent activity against HDACs and tumor cells, also released the most NO among these tested compounds.

(**Figure 5** should be listed here)

In Vitro Antiproliferative Assay with Hemoglobin.

In order to verify that the proliferation of tumor cells were also inhibited by NO generated

from our compounds, we further examined the anti-proliferation effects of **5c** in the presence or absence of NO scavenger, hemoglobin (Hb). HEL cells were pretreated with the indicated concentrations of NO scavenger hemoglobin (0, 2.5, 5, 10 and 20 μM) for 1 hour and then treated by 2 μM of **5c** for 24 hours. The results were expressed as the percentage of growth inhibition relative to the control cells in Figure 6. It was observed that **5c** remarkably inhibited the growth of HEL cells and this inhibitory effect was diminished by pretreatment with hemoglobin in a dose-dependent manner. These results demonstrated that NO produced by **5c** contributed in part to its inhibition of tumor cell proliferation, which validated our compound design strategy.

(**Figure 6** should be listed here)

Induction of Apoptosis in Vitro.

As the fact that high levels of NO act as a tumor cell apoptosis inducer, the ability of **5c** as NO donor to induce tumor cell apoptosis was tested and compared with that of SAHA. HEL cells were treated with a variable level of **5c**, SAHA and **2** for 24 h. The cells were harvested and stained with 7-aminoactinomycin D (7-AAD) and annexin-V, and the percentage of apoptotic cells were determined by flow cytometry analysis. Notably, it was found that the ability of **5c** to induce apoptosis was stronger than that of SAHA in HEL cells (Figure 7, A), and the apoptosis rate was in a dose-dependent manner (Figure 7, B).

(**Figure 7** should be listed here)

Cell Cycle Arrest Analysis.

The effect of **5c** on the various phases of cell cycle progression was tested in HEL cells (Figure 8). In comparison to the control population, the cell cycle data clearly showed **5c** arrested HEL cells mainly in G1 phase (90.24%), which was stronger than that of SAHA (79.98%).

(**Figure 8** should be listed here)

In Vivo Antitumor Activity.

Compound **5c** was further evaluated for its in vivo antitumor efficacy in HEL xenograft mouse model. Compound **5c** (100 mg/kg/day, 120 mg/kg/day) and SAHA (120 mg/kg/day) were dosed orally by gavage for 21 consecutive days. Tumor growth inhibition (TGI) and relative increment ratio (T/C) were calculated as described previously[31] at the end of treatment to reveal the antitumor effects in tumor weight and tumor volume, respectively.

In the HEL xenograft model, compound **5c** exhibited dose-dependent antitumor activity, and at the same dosage of 120 mg/kg/day, compound **5c** demonstrated superior antitumor activity (TGI = 48%, T/C = 39%) to that of the reference compound SAHA (TGI = 39%, *T/C* = 46%). The tumor growth curve depicted in Figure 9 and the final tumor tissue size visualized in Figure 10 also explicitly showed an excellent antitumor potency of **5c**. Importantly, mice treated by higher dose of **5c** (120 mg/kg) showed no significant body weight loss (Figure 11) and no evidence of liver or spleen toxicity.

(**Figure 9** should be listed here)

(**Figure 10** should be listed here)

(**Figure 11** should be listed here)

In Vitro HDAC Isoform Selectivity of 5c.

In order to explore its HDAC isoform selective profile, **5c** was tested for its inhibitory activity of HDAC1, HDAC2, HDAC3, HDAC4, HDAC6, HDAC8 and HDAC 11 (Table 4). From the results we found that at the molecular level, compound **5c** exhibited remarkable selectivity for HDAC6 over other isoforms.

(**Table 4** should be listed here)

Western Blot Analysis.

In order to investigate its HDAC isoform selectivity in cellular environment, compound **5c** was further evaluated in western blot assays to determine acetylated protein levels (Figure 12). The results in Figure 12A showed that at its very low concentration of 12.5 nM, compound **5c** still could dramatically increase cellular level of ac-tubulin, the substrate of HDAC6, which was in line with its highly potent HDAC6 inhibitory activity (IC50 of 7 nM). However, **5c** could also effectively increase cellular levels of AcHH3 and AcHH4, which were the main nuclear substrates of HDAC1 and HDAC2. This is not very surprising because **5c** could release NO

effectively and some research showed that NO not only could inhibit the enzyme activity[24] and chromatin binding of HDAC2 by S-nitrosylation,[26] but also could minimally inhibit HDAC1 by an S-nitrosylation-independent mechanism,[24] Moreover, our results also showed that **5c** could decrease the cellular level of HDAC2 at higher concentrations (1 μM and 10 μM, Figure 12B), which could also be attributed to release NO because the NO scavenger PTIO could recover the cellular level of HDAC2 (Figure 12C). Additional research to elucidate the mechanism on how NO affecting cellular levels of HDAC2 is warranted.

(**Figure 12** should be listed here)

■ CONCLUSION

In the present research, a novel series of compounds capable to simultaneously release NO and inhibit HDACs were designed and synthesized for the treatment of cancer based on the "multifunctional drugs" approach. All synthesized compounds were evaluated for their HDAC inhibitory potency against Hela cell nuclear extracts and for their antiproliferative effects against several tumor cell lines. Several representative compounds were evaluated in HEL cell line and displayed potent NO releasing activity with compound **5c** being the most potent one. Pretreatment of HEL cells with NO scavenger hemoglobin could moderately reduce the antiproliferative activity of **5c** demonstrated the additive effect between NO release and HDAC inhibition. Further mechanistic studies revealed that **5c** induced a much stronger apoptotic effect and G1 phase arrest in HEL cells than SAHA, which was in line with their abilities to inhibit

HDAC and to generate NO. Because of its very promising in vitro activity, compound **5c** was progressed to a HEL xenograft model and exhibited greater oral antitumor potency than SAHA in a dose-dependent manner. It is worth noting that compound **5c** was a remarkably HDAC6 selective inhibitor in the molecular level, which could be used as a design template for HDAC6 selective inhibitors. Taken together, compound **5c,** a very potent HDAC inhibitor with NO releasing activity was discovered, which deserves further research and development as a promising therapeutic agent for hematologic malignancies.

■ EXPERIMENTAL SECTION

Chemistry Materials and Methods. All commercially available starting materials, reagents, and solvents were used without further purification unless otherwise stated. All reactions were monitored by TLC with 0.25 mm silica gel plates (60GF-254). UV light, iodine stain, and ferric chloride were used to visualize the spots. Silica gel or C18 silica gel was used for column chromatography purification. ^{1}H NMR and ^{13}C spectra were recorded on a Bruker DRX spectrometer at 600 MHz, δ in parts per million and *J* in hertz, using TMS as an internal standard. High-resolution mass spectra were conducted by Shandong Analysis and Test Center in Ji'nan, China. ESI-MS spectra were recorded on an API 4000 spectrometer. Melting points were determined uncorrected on an electrothermal melting point apparatus. All tested compounds are >95% pure by HPLC analysis, performed on a Agilent 1100 HPLC instrument using an 5 μm ODS HYPERSIL column (4.6 mm×250 mm) according to the following methods. All target compounds were eluted with 35% acetonitrile/65% water (containing 0.1% acetic acid) over 20

min, with detection at 254 nm and a flow rate of 1.0 mL/min.

Synthesis of compound 2 (*3,4-bis(phenylsulfonyl)-1,2,5-oxadiazole 2-oxide*):

To a solution of (phenylthio)acetic acid (10.0 g， 55.0 mmol) in glacial acetic acid (16 mL), aqueous H_2O_2 (30%, 13.6 mL) was added at 0℃, after 1.0 h of stirring at room temperature, the mixture was continued stirred at 80℃ for 3 h after additional of fuming nitric acid (24 mL) controlling the inner temperature lower than 20℃. The reaction was checked by TLC and the mixture was cooled after it reacted completely, and then the compound **2** was collected by filtration and dry under vacuum as a white solid (Yield: 56%). ^{1}H NMR (400 MHz, $CDCl_3$)[19] δ 8.20 (t, *J* = 7.4 Hz, 4H), 7.83 (dd, *J* = 14.3, 7.3 Hz, 2H), 7.69 (dt, *J* = 16.1, 8.2 Hz,4H).

General procedure for the preparation of compounds (3a-3o)

4-(4-hydroxybutoxy)-3-(phenylsulfonyl)-1,2,5-oxadiazole 2-oxide (3a)*:* To a solution of compound **2** (1.1 g, 2.7 mmol) in 10 mL THF 1,4-Butanediol was added (1.2 mL, 11.4 mmol) at approximately 5℃, followed by dropwise addition of 2.5 N aqueous NaOH (1 mL) followed by 30 min stirring. The solution was concentrated under vacuum at room temperature. The residue was extracted with EtOAc three times (3×50 mL) and washed twice with water and brine. The combined organic layers were dried by anhydrous Na_2SO_4, and evaporated under vacuum to give a residue that was purified by silica-gel column chromatography tresulting in a white solid product. (Yield:71%). ^{1}H NMR (400 MHz, $CDCl_3$)[31] δ 8.05 (d, *J* = 7.7 Hz, 2H), 7.76 (t, *J* = 7.3 Hz, 1H), 7.62 (t, *J* = 7.6 Hz, 2H), 4.47 (t, *J* = 6.1 Hz, 2H), 3.76 (t, *J* = 6.1 Hz, 2H), 2.07 – 1.91

(m, 2H), 1.82 – 1.71 (m, 2H), 1.62 (s, 1H).

4-((5-hydroxypentyl)oxy)-3-(phenylsulfonyl)-1,2,5-oxadiazole 2-oxide (3b)*:* white solid. (Yield: 66%). ^{1}H NMR (600 MHz, d_6-DMSO) [32] δ 8.02 (d, *J* = 7.7 Hz, 2H), 7.91 (t, *J* = 7.4 Hz, 1H), 7.76 (t, *J* = 7.5 Hz, 2H), 4.39 (t, *J* = 6.2 Hz, 2H), 3.42 (t, *J* = 6.2 Hz, 2H), 1.79 – 1.72 (m, 2H), 1.50 – 1.44 (m, 2H), 1.42 – 1.37 (m, 2H).

4-((6-hydroxyhexyl)oxy)-3-(phenylsulfonyl)-1,2,5-oxadiazole 2-oxide (3c)*:* white solid. (Yield: 73%). ^{1}H NMR (600 MHz, d_6-DMSO)[32] δ 8.02 (d, *J* = 7.7 Hz, 2H), 7.91 (t, *J* = 7.3 Hz, 1H), 7.76 (t, *J* = 7.8 Hz, 2H), 4.38 (t, *J* = 6.3 Hz, 2H), 3.98 (t, *J* = 6.7 Hz, 2H), 1.79 – 1.71 (m, 2H), 1.58 – 1.52 (m, 2H), 1.35 (d, *J* = 3.1 Hz, 2H), 1.29 (d, *J* = 3.1 Hz, 2H).

4-((7-hydroxyheptyl)oxy)-3-(phenylsulfonyl)-1,2,5-oxadiazole 2-oxide (3d)*:* white solid. (Yield: 66%). ^{1}H NMR (600 MHz, $CDCl_3$) δ 8.05 (d, *J* = 7.8 Hz, 2H), 7.74 (t, *J* = 7.5 Hz, 1H), 7.61 (t, *J* = 7.7 Hz, 2H), 4.42 (t, *J* = 6.5 Hz, 2H), 3.66 (t, *J* = 6.6 Hz, 2H), 1.91 – 1.84 (m, 2H), 1.59 (dd, *J* = 13.0, 6.5 Hz, 2H), 1.50 – 1.46 (m, 2H), 1.42 (dd, *J* = 6.5, 3.5 Hz, 4H). ^{13}C NMR (151 MHz, $CDCl_3$) δ 159.2, 138.4, 135.7, 129.8, 129.3, 128.7, 128.0, 110.6, 71.7, 63.0, 32.7, 29.0, 28.4, 25.7, 25.7. ESI-MS $[M+H]^+$ m/z: 357.1.

4-((8-hydroxyoctyl)oxy)-3-(phenylsulfonyl)-1,2,5-oxadiazole 2-oxide (3e)*:* white solid. (Yield: 71%). ^{1}H NMR (600 MHz, $CDCl_3$) δ 8.04 (d, *J* = 7.8 Hz, 2H), 7.75 (t, *J* = 7.5 Hz, 1H), 7.61 (t, *J* = 7.6 Hz, 2H), 4.40 (t, *J* = 6.5 Hz, 2H), 3.62 (s, 2H), 1.88 – 1.82 (m, 2H), 1.65 – 1.49 (m, 8H), 1.44 (dd, *J* = 13.6, 6.4 Hz, 2H). ^{13}C NMR (151 MHz, $CDCl_3$) δ 159.1, 138.1, 135.6, 129.6, 129.2,

128.5, 127.8, 110.5, 71.6, 62.9, 32.7, 29.2, 29.0, 28.4, 25.6, 25.6, 25.5. ESI-MS $[M+H]^+$ m/z: 371.1.

4-(2-(2-hydroxyethoxy)ethoxy)-3-(phenylsulfonyl)-1,2,5-oxadiazole 2-oxide (3f)*:* white solid. (Yield: 56%). ^{1}H NMR (400 MHz, $CDCl_3$) [32] δ 8.06 (d, *J* = 7.7 Hz, 2H), 7.75 (t, *J* = 7.5 Hz, 1H), 7.61 (t, *J* = 7.8 Hz, 2H), 4.62 – 4.51 (m, 2H), 3.97 – 3.89 (m, 2H), 3.81 – 3.74 (m, 2H), 3.72 – 3.67 (m, 2H).

4-(3-hydroxy-2,2-dimethylpropoxy)-3-(phenylsulfonyl)-1,2,5-oxadiazole 2-oxide (3g)*:* white solid. (Yield: 80%).^{1}H NMR (400 MHz, $CDCl_3$) δ 8.04 (d, *J* = 8.0 Hz, 2H), 7.75 (t, *J* = 7.1 Hz, 1H), 7.61 (t, *J* = 7.7 Hz, 2H), 4.23 (s, 2H), 3.55 (s, 2H), 1.05 (s, 6H). ^{13}C NMR (400 MHz, $CDCl_3$) δ 153.5, 137.4, 132.6, 132.1, 127.6, 76.7, 69.6, 37.1, 19.4. ESI-MS $[M+H]^+$ m/z: 329.1.

(E)-4-((4-hydroxybut-2-en-1-yl)oxy)-3-(phenylsulfonyl)-1,2,5-oxadiazole 2-oxide (3h)*:* white solid. (Yield: 70%). ^{1}H NMR (600 MHz, $CDCl_3$) δ 8.12 – 8.02 (m, 2H), 7.96 – 7.87 (m, 1H), 7.81 – 7.69 (m, 2H), 5.98 – 5.77 (m, 2H), 4.68 (dd, *J* = 11.5, 1.0 Hz, 2H), 4.23 – 4.11 (m, 2H). ^{13}C NMR (400 MHz, $CDCl_3$) δ 155.5, 137.4, 132.6, 132.1, 131.7, 128.1, 127.6, 69.6, 63.3. ESI-MS $[M+H]^+$ m/z: 313.0.

4-(2-(2-(2-hydroxyethoxy)ethoxy)ethoxy)-3-(phenylsulfonyl)-1,2,5-oxadiazole 2-oxide (3i)*:* white solid. (Yield:58%). ^{1}H NMR (600 MHz, $CDCl_3$)[19] δ 8.03 (d, *J* = 7.6 Hz, 2H), 7.90 (d, *J* = 7.5 Hz, 1H), 7.76 (t, *J* = 7.9 Hz, 2H), 4.53 – 4.50 (m, 2H), 3.81 – 3.79 (m, 2H), 3.64 – 3.61 (m, 2H), 3.57 – 3.54 (m, 2H), 3.49 (d, *J* = 5.3 Hz, 2H), 3.43 (d, *J* = 5.0 Hz, 2H).

4-(4-(hydroxymethyl)phenoxy)-3-(phenylsulfonyl)-1,2,5-oxadiazole 2-oxide (3j)*:* white solid. (Yield: 68%). ^{1}H NMR (600 MHz, d_6-DMSO)[19] δ 8.06 (d, *J* = 7.9 Hz, 2H), 7.93 (t, *J* = 7.3 Hz, 1H), 7.78 (t, *J* = 7.6 Hz, 2H), 7.43 (d, *J* = 8.3 Hz, 2H), 7.37 (d, *J* = 8.3 Hz, 2H), 5.27 (t, *J* = 5.7 Hz, 1H).

4-(3-(hydroxymethyl)phenoxy)-3-(phenylsulfonyl)-1,2,5-oxadiazole 2-oxide (3k)*:* white solid. (Yield: 74%). ^{1}H NMR (600 MHz, d_6-DMSO)[19] δ 8.05 (d, *J* = 7.7 Hz, 2H), 7.91 (t, *J* = 7.5 Hz, 1H), 7.77 (t, *J* = 7.8 Hz, 2H), 7.43 (t, *J* = 7.9 Hz, 1H), 7.35 (s, 1H), 7.27 (dd, *J* = 11.4, 9.1 Hz, 2H), 5.27 (t, *J* = 5.5 Hz, 1H), 4.54 (d, *J* = 5.1 Hz, 2H).

4-(4-(hydroxymethyl)-2-methoxyphenoxy)-3-(phenylsulfonyl)-1,2,5-oxadiazole 2-oxide (3l)*:* white solid. (Yield: 67%). ^{1}H NMR (600 MHz, $CDCl_3$) δ 8.09 (d, *J* = 8.2 Hz, 2H), 7.95 (t, *J* = 7.4 Hz, 1H), 7.81 (t, *J* = 7.7 Hz, 2H), 7.36 (d, *J* = 8.2 Hz, 1H), 7.17 (s, 1H), 6.98 (d, *J* = 8.2 Hz, 1H), 5.31 (d, *J* = 5.7 Hz, 1H), 4.53 (d, *J* = 5.8 Hz, 2H), 3.72 (s, 3H). ^{13}C NMR (400 MHz, $CDCl_3$) δ 155.3, 150.9, 137.4, 136.6, 132.6, 132.1, 128.2, 127.6, 120.7, 63.2, 39.4. ESI-MS $[M+H]^+$ m/z: 379.1.

4-(4-(2-hydroxyethyl)phenoxy)-3-(phenylsulfonyl)-1,2,5-oxadiazole 2-oxide (3m)*:* colorless oil. (Yield: 61%). ^{1}H NMR (600 MHz, $CDCl_3$) δ 8.06 (d, *J* = 8.1 Hz, 2H), 7.92 (t, *J* = 7.4 Hz, 1H), 7.77 (t, *J* = 7.6 Hz, 2H), 7.32 (q, *J* = 8.6 Hz, 4H), 4.66 (t, *J* = 5.1 Hz, 1H), 3.64 (dd, *J* = 12.4, 6.3 Hz, 2H), 2.76 (t, *J* = 6.8 Hz, 2H). ^{13}C NMR (400 MHz, $CDCl_3$) δ 154.3, 137.4, 132.6, 132.1, 127.6, 72.6, 70.4, 70.0, 66.6, 61.0. ESI-MS $[M+H]^+$ m/z: 363.1.

4-((2-(hydroxymethyl)-2-methylpentyl)oxy)-3-(phenylsulfonyl)-1,2,5-oxadiazole 2-oxide (3n)*:* colorless oil. (Yield: 63%). ^{1}H NMR (600 MHz, $CDCl_3$) δ 8.08 – 8.01 (m, 2H), 7.95 – 7.86 (m, 1H), 7.76 – 7.68 (m, 2H), 4.27 (dd, *J* = 172.0, 24.7 Hz, 2H), 3.42 (dd, *J* = 127.1, 24.7 Hz, 2H), 1.49 (s, 1H), 1.45 – 1.33 (m, 4H), 0.95 (d, *J* = 8.4 Hz, 3H), 0.91 – 0.83 (m, 3H). ^{13}C NMR (400 MHz**,** $CDCl_3$) δ 153.5, 137.4, 132.6, 132.1, 127.6, 73.7, 69.9, 38.8, 34.1, 20.3 17.1, 14.7. ESI-MS $[M+H]^+$ m/z: 357.1.

General procedure for the preparation of compounds (4a-4n)

4-(3-carboxypropoxy)-3-(phenylsulfonyl)-1,2,5-oxadiazole 2-oxide (4a)*:* To a solution of **3**(680 mg，2.2 mmol) in 10 mL acetone, *Jones* reagent (1.1 mL) was added at 0-5℃.This mixture was stirred at r.t. for 10 h. The precipitate was filtered off and acetone was removed in vacuo, and then EtOAc (3×50 mL) was added,the organic portion was washed with water and brine, and dried by anhydrous Na_2SO_4. The crude product was obtained by removing EtOAc and purified by silica chromatography column (P:E=3:1) to get the product. white solid. (Yield: 81%). ^{1}H NMR (400 MHz, $CDCl_3$) δ 8.05 (d, *J* = 7.6 Hz, 2H), 7.76 (t, *J* = 7.4 Hz, 1H), 7.62 (t, *J* = 7.8 Hz, 2H), 4.50 (t, *J* = 6.0 Hz, 2H), 2.60 (t, *J* = 7.0 Hz, 2H), 2.26 – 2.19 (m, 2H), 2.17 (s, 1H). ^{13}C NMR (400 MHz**,** $CDCl_3$) δ 177.2, 154.3, 137.4, 132.6, 132.1, 127.6, 68.0, 31.8, 24.3. ESI-MS $[M+H]^+$ m/z: 329.0.

4-(4-carboxybutoxy)-3-(phenylsulfonyl)-1,2,5-oxadiazole 2-oxide (4b)*:* white solid. (Yield: 80%). ^{1}H NMR (600 MHz, $CDCl_3$) δ 12.09 (s, 1H), 8.02 (d, *J* = 8.0 Hz, 2H), 7.90 (t, *J* = 7.4 Hz,

1H), 7.75 (t, *J* = 7.6 Hz, 2H), 4.40 (t, *J* = 6.0 Hz, 2H), 2.30 (t, *J* = 7.3 Hz, 2H), 1.82 – 1.74 (m, 2H), 1.62 (t, *J* = 6.4 Hz, 2H). ^{13}C NMR (400 MHz, $CDCl_3$) δ 177.2, 154.3, 137.4, 132.6, 132.1, 127.6, 69.3, 34.5, 28.8, 22.1. ESI-MS $[M+H]^+$ m/z: 343.0.

4-((5-carboxypentyl)oxy)-3-(phenylsulfonyl)-1,2,5-oxadiazole 2-oxide (4c)*:* white solid. (Yield: 73%). ^{1}H NMR (600 MHz, d_6-DMSO) δ 12.04 (s, 1H), 8.04 – 8.00 (m, 2H), 7.91 (t, *J* = 7.4 Hz, 1H), 7.76 (t, *J* = 7.9 Hz, 2H), 4.38 (t, *J* = 6.2 Hz, 2H), 2.24 (t, *J* = 7.3 Hz, 2H), 1.79 – 1.71 (m, 2H), 1.58 – 1.54 (m, 2H), 1.38 (dd, *J* = 15.3, 8.0 Hz, 2H). ^{13}C NMR (400 MHz, $CDCl_3$) δ 177.2, 154.3, 137.4, 132.6, 132.1, 127.6, 69.3, 34.5, 29.3, 25.9, 24.9. ESI-MS $[M+H]^+$ m/z: 357.1.

4-((6-carboxyhexyl)oxy)-3-(phenylsulfonyl)-1,2,5-oxadiazole 2-oxide (4d)*:* white solid. (Yield: 83%). ^{1}H NMR (600 MHz, $CDCl_3$) δ 11.58 (s, 1H), 8.07 (d, *J* = 8.0 Hz, 2H), 7.78 (t, *J* = 7.5 Hz, 1H), 7.64 (t, *J* = 7.8 Hz, 2H), 4.43 (t, *J* = 6.4 Hz, 2H), 2.38 (d, *J* = 7.4 Hz, 2H), 1.94 – 1.85 (m, 2H), 1.69 (dd, *J* = 14.8, 7.3 Hz, 4H), 1.48 – 1.43 (m, 2H). ^{13}C NMR (400 MHz, $CDCl_3$) δ 180.0, 159.0, 138.1, 135.6, 129.7, 129.2, 128.5, 127.8, 110.5, 71.4, 33.8, 28.5, 28.2, 25.3, 24.2. ESI-MS $[M+H]^+$ m/z: 371.1.

4-((7-carboxyheptyl)oxy)-3-(phenylsulfonyl)-1,2,5-oxadiazole 2-oxide (4e)*:* white solid. (Yield: 79%). ^{1}H NMR (600 MHz, $CDCl_3$) δ 8.06 (d, *J* = 7.9 Hz, 2H), 7.77 (t, *J* = 7.4 Hz, 1H), 7.62 (d, *J* = 7.8 Hz, 2H), 4.42 (t, *J* = 6.5 Hz, 2H), 2.37 – 2.34 (m, 2H), 1.91 – 1.84 (m, 2H), 1.68 – 1.58 (m, 8H). ^{13}C NMR (151 MHz, $CDCl_3$) δ 179.6, 159.0, 138.2, 135.5, 129.6, 129.2, 128.5, 127.8, 71.6, 33.9, 28.8, 28.7, 28.3, 25.4, 24.5. ESI-MS $[M+H]^+$ m/z: 385.1.

4-(2-(carboxymethoxy)ethoxy)-3-(phenylsulfonyl)-1,2,5-oxadiazole 2-oxide (4f)*:* white solid. (Yield: 85%). ^{1}H NMR (600 MHz, $CDCl_3$) δ 8.07 (s, 2H), 7.74 (s, 1H), 7.61 (s, 2H), 4.61 (s, 2H), 4.28 (s, 2H), 4.02 (s, 2H). ^{13}C NMR (400 MHz, $CDCl_3$) δ 173.8, 154.3, 137.4, 132.6, 132.1, 127.6, 69.8, 67.9, 66.6. ESI-MS $[M+H]^+$ m/z:345.0.

4-(2-carboxy-2-methylpropoxy)-3-(phenylsulfonyl)-1,2,5-oxadiazole 2-oxide (4g)*:* white solid. (Yield: 79%). ^{1}H NMR (600 MHz, $CDCl_3$) δ 8.12 – 7.95 (m, 2H), 7.79 – 7.70 (m, 1H), 7.60 (t, *J* = 7.8 Hz, 2H), 4.43 (s, 2H), 1.41 (s, 6H). ^{13}C NMR (400 MHz, $CDCl_3$) δ 182.7, 153.5, 137.4, 132.6, 132.1, 127.6, 77.0, 43.3, 23.4. ESI-MS $[M+H]^+$ m/z:343.0.

(E)-4-((3-carboxyallyl)oxy)-3-(phenylsulfonyl)-1,2,5-oxadiazole 2-oxide (4h)*:* white solid. (Yield: 88%). ^{1}H NMR (600 MHz, $CDCl_3$) δ 12.80 (s, 1H), 8.04 (d, *J* = 8.1 Hz, 2H), 7.90 (t, *J* = 7.4 Hz, 1H), 7.75 (t, *J* = 7.6 Hz, 2H), 6.54 – 6.47 (m, 1H), 5.97 (d, *J* = 11.6 Hz, 1H), 5.48 (dd, *J* = 4.7, 2.2 Hz, 2H). ^{13}C NMR (400 MHz, $CDCl_3$) δ 171.8, 155.5, 149.5, 137.4, 132.6, 132.1, 127.6, 119.7, 68.3. ESI-MS $[M+H]^+$ m/z:327.0.

4-(2-(2-(carboxymethoxy)ethoxy)ethoxy)-3-(phenylsulfonyl)-1,2,5-oxadiazole 2-oxide (4i)*:* white solid. (Yield: 82%). ^{1}H NMR (600 MHz, $CDCl_3$) δ 8.10 – 8.00 (m, 2H), 7.98 – 7.88 (m, 1H), 7.78 – 7.70 (m, 2H), 4.33 (s, 2H), 4.31 (t, *J* = 7.8 Hz, 2H), 3.77 (t, *J* = 7.8 Hz, 2H), 3.52 (s, 4H). ^{13}C NMR (400 MHz, $CDCl_3$) δ 173.8, 154.3, 137.4, 132.6, 132.1, 127.6, 70.4, 70.0, 69.7, 67.9, 66.6. ESI-MS $[M+H]^+$ m/z:389.1.

4-(4-carboxyphenoxy)-3-(phenylsulfonyl)-1,2,5-oxadiazole 2-oxide (4j)*:* white solid. (Yield:

78%). ^{1}H NMR (600 MHz, $CDCl_3$) δ 13.11 (s, 1H), 8.05 (t, *J* = 8.0 Hz, 4H), 7.92 (t, *J* = 7.5 Hz, 1H), 7.77 (t, *J* = 7.9 Hz, 2H), 7.56 (d, *J* = 8.8 Hz, 2H). ^{13}C NMR (400 MHz, $CDCl_3$) δ 168.8, 157.7, 155.3, 137.4, 132.6, 132.1, 129.9, 127.6, 126.7, 120.3. ESI-MS $[M+H]^+$ m/z:363.0.

4-(3-carboxyphenoxy)-3-(phenylsulfonyl)-1,2,5-oxadiazole 2-oxide (4k)*:* white solid. (Yield: 81%). ^{1}H NMR (600 MHz, $CDCl_3$) δ 13.34 (s, 1H), 8.07 (d, *J* = 7.8 Hz, 2H), 7.99 (s, 1H), 7.92 (t, *J* = 7.4 Hz, 2H), 7.77 (t, *J* = 7.8 Hz, 2H), 7.73 – 7.69 (m, 1H), 7.64 (t, *J* = 7.9 Hz, 1H). ^{13}C NMR (400 MHz, $CDCl_3$) δ 168.01, 155.3, 152.2, 137.4, 132.6, 132.1, 130.0, 128.5, 127.6, 126.4, 126.3, 122.3. ESI-MS $[M+H]^+$ m/z:363.0.

4-(4-carboxy-2-methoxyphenoxy)-3-(phenylsulfonyl)-1,2,5-oxadiazole 2-oxide (4l)*:* white solid. (Yield: 73%). ^{1}H NMR (600 MHz, $CDCl_3$) δ 13.20 (s, 1H), 8.08 (d, *J* = 7.6 Hz, 2H), 7.95 (t, *J* = 7.5 Hz, 1H), 7.81 (t, *J* = 7.9 Hz, 2H), 7.69 (d, *J* = 1.4 Hz, 1H), 7.64 (dd, *J* = 8.4, 1.6 Hz, 1H), 7.57 (d, *J* = 8.3 Hz, 1H), 3.75 (s, 3H). ^{13}C NMR (400 MHz, $CDCl_3$) δ 168.1, 156.2, 149.0, 146.8, 137.4, 132.6, 132.1, 127.6, 125.1, 122.2, 121.9, 117.6, 56.8. ESI-MS $[M+H]^+$ m/z:393.0.

4-(4-(carboxymethyl)phenoxy)-3-(phenylsulfonyl)-1,2,5-oxadiazole 2-oxide (4m)*:* colorless oil. (Yield: 88%). ^{1}H NMR (600 MHz, $CDCl_3$) δ 12.33 (s, 1H), 8.04 (d, *J* = 7.8 Hz, 2H), 7.92 (t, *J* = 7.4 Hz, 1H), 7.77 (t, *J* = 7.7 Hz, 2H), 7.37 (q, *J* = 8.8 Hz, 4H), 3.64 (s, 2H). ^{13}C NMR (400 MHz, $CDCl_3$) δ 174.9, 155.3, 147.0, 137.4, 132.6, 132.1, 131.1, 127.6, 126.6, 118.9, 44.4. ESI-MS $[M+H]^+$ m/z:376.0.

4-((2-carboxy-2-methylpentyl)oxy)-3-(phenylsulfonyl)-1,2,5-oxadiazole 2-oxide (4n)*:* colorless

oil. (Yield: 86%). ^{1}H NMR (600 MHz, $CDCl_3$) δ 8.07 (d, *J* = 8.9 Hz, 2H), 7.93 (t, *J* = 7.5 Hz, 1H), 7.75 (t, *J* = 7.4 Hz, 2H), 4.85 (dd, *J* = 283.1, 12.4 Hz, 2H), 1.67 (dt, *J* = 98.5, 7.7 Hz, 2H), 1.46 – 1.36 (m, 2H), 0.97 (s, 3H), 0.89 (t, *J* = 6.6 Hz, 3H). ^{13}C NMR (400 MHz, $CDCl_3$) δ 179.7, 153.5, 137.4, 132.6, 132.1, 127.6, 73.5, 44.8, 40.1, 26.4, 17.2, 14.7. ESI-MS $[M+H]^+$ m/z: 370.1.

The preparation of compound 6 ***(4-(4-formylphenoxy)-3-(phenylsulfonyl)-1,2,5-oxadiazole 2-oxide)****:* To a stirred suspension of PCC (648 mg, 3 mmol) in DCM at 0℃, compound **3j** (600 mg, 1.8 mmol) was added, and the solution was stirred at 0℃ for 5 h. The solution was concentrated under vacuum at room temperature. The residue was extracted with EtOAc three times (3×50 mL) and washed twice with water and brine. The combined organic layers were dried by anhydrous Na_2SO_4, and evaporated under vacuum to give a residue that was purified by silica-gel column chromatography (P:E=3:1) to get the product as a white solid. (Yield: 68%). ^{1}H NMR (600 MHz, d_6-DMSO)[19] δ 9.98 (s, 1H), 7.95 (d, *J* = 8.5 Hz, 2H), 7.91 (d, *J* = 7.7 Hz, 2H), 7.85 (t, *J* = 7.5 Hz, 1H), 7.70 (t, *J* = 7.9 Hz, 2H), 7.29 (d, *J* = 8.5 Hz, 2H).

The preparation of compound 7 ***((E)-4-(4-(2-carboxyvinyl)phenoxy)-3-(phenylsulfonyl)-1,2,5-oxadiazole 2-oxide)****:* To a solution of propandioic acid (710 mg, 2.4 mmol) in pyridine, Pyrrolidine (0.03 mL) was added and the mixture was stirred at room temperature for 20 minutes. After that, the compound **6** (750 mg, 2.4 mmol)was added and the reaction mixture was heated to 100℃ in reflux for 3h. Pyridine was removed and the residue was extracted with EtOAc (3×50 mL) and washed twice with water and brine. The organic portion was dried by anhydrous Na_2SO_4. The crude product

was obtained by removing EtOAc and purified by silica chromatography column (P:E=3:1) to get the product as white solid. (Yield: 80%). ^{1}H NMR (600 MHz, d_6-DMSO) δ 12.47 (s, 1H), 8.05 (d, *J* = 7.8 Hz, 2H), 7.93 (t, *J* = 7.4 Hz, 1H), 7.83 (d, *J* = 8.7 Hz, 2H), 7.77 (t, *J* = 7.8 Hz, 2H), 7.63 (d, *J* = 16.0 Hz, 1H), 7.48 (d, *J* = 8.7 Hz, 2H), 6.57 (d, *J* = 16.0 Hz, 1H). ^{13}C NMR (400 MHz, d_6-DMSO) δ 170.5, 155.3, 153.2, 143.7, 137.4, 132.6, 132.1, 131.9, 130.9, 127.6, 121.7, 115.0. ESI-MS $[M+H]^+$ m/z:389.0.

General procedure for the preparation of compounds (5a-o)

4-(4-(hydroxyamino)-4-oxobutoxy)-3-(phenylsulfonyl)-1,2,5-oxadiazole 2-oxide (5a): To a solution of compound **4a** (1.2 g, 3.8 mmol) in dried THF, Isobutyl chlorocarbonate (0.9 mL, 3.9 mmol) was added by drop at 0℃, after stirring 0.5h, triethylamine (0.9 mL, 2.5 mmol) was added dropwise at 0℃. The mixture was further stirred for additional 1 h at room temperature and solid precipitates were filtered resulting in the first filtrate. Potassium hydroxide (319.2 mg, 5.7 mmol) and hydroxylamine hydrochloride (396.1 mg, 5.7 mmol) were dissolved in anhydrous menthol completely and the residue was filtered to get the second filtrate. The first filtrate was added into the second filtrate and the mixture was stirred for additional 4 h at room temperature under nitrogen atmosphere. Ferric trichloride was the color-producing reagent. THF and menthol were removed after the pH of the reacted solution was adjusted to 3.0 with 2N HCl. And then the residue was extracted with EtOAc.The organic portion was dried by anhydrous Na_2SO_4. The crude product was obtained by removing EtOAc and purified by silica chromatography column (P:E=3:1) to get the product. white solid. (Yield: 73%). M.p. 139-141℃. ^{1}H NMR (600 MHz,

d_6-DMSO) δ 10.51 (s, 1H), 8.80 (s, 1H), 8.03 (d, J = 8.2 Hz, 2H), 7.89 (t, J = 7.4 Hz, 1H), 7.74 (t, J = 7.5 Hz, 2H), 4.40 (t, J = 6.2 Hz, 2H), 2.13 (t, J = 7.3 Hz, 2H), 2.02 – 1.97 (m, 2H). ^{13}C NMR (400 MHz, d_6-DMSO) δ 168.4, 159.1, 137.3, 136.4, 130.2, 128.6, 128.5, 110.7, 71.0, 28.3, 24.4. HRMS (ESI) m/z calcd for $C_{12}H_{14}N_3O_7S$ $[M+H]^+$ 344.0547, found 344.0548.

4-((5-(hydroxyamino)-5-oxopentyl)oxy)-3-(phenylsulfonyl)-1,2,5-oxadiazole 2-oxide (5b)*:* white solid. (Yield: 68%). M.p. 119-121℃. ^{1}H NMR (600 MHz, d_6-DMSO) δ 10.39 (s, 1H), 8.74 (s, 1H), 8.02 (d, *J* = 7.9 Hz, 2H), 7.90 (t, *J* = 7.3 Hz, 1H), 7.76 (t, *J* = 7.8 Hz, 2H), 4.38 (t, *J* = 6.1 Hz, 2H), 1.79 – 1.71 (m, 2H), 1.66 – 1.58 (m, 3H), 1.53 (t, *J* = 6.8 Hz, 2H). ^{13}C NMR (400 MHz, d_6-DMSO) δ 169.2, 159.3, 137.6, 136.6, 130.6, 128.8, 110.9, 71.5,32.1, 27.9, 21. 8. HRMS (ESI) m/z calcd for $C_{13}H_{16}N_3O_7S$ $[M+H]^+$ 358.0703, found 358.0705.

4-((6-(hydroxyamino)-6-oxohexyl)oxy)-3-(phenylsulfonyl)-1,2,5-oxadiazole 2-oxide (5c)*:* white solid. (Yield: 62%). M.p. 135-137℃. ^{1}H NMR (600 MHz, d_6-DMSO) δ 10.37 (s, 1H), 8.70 (s, 1H), 8.04 – 7.99 (m, 2H), 7.90 (t, *J* = 7.5 Hz, 1H), 7.76 (t, *J* = 7.9 Hz, 2H), 4.37 (t, *J* = 6.3 Hz, 2H), 1.97 (t, *J* = 7.4 Hz, 2H), 1.78 – 1.69 (m, 2H), 1.57 – 1.51 (m, 2H), 1.32 (dt, *J* = 15.3, 7.7 Hz, 2H). ^{13}C NMR (400 MHz, d_6-DMSO) δ 169.4, 159.3, 137.6, 136.6, 130.5, 128.8, 110.9, 71.8, 32.6, 28.1, 25.2, 25.1. HRMS (ESI) m/z calcd for $C_{14}H_{18}N_3O_7S$ $[M+H]^+$ 372.0860, found 372.0866.

4-((7-(hydroxyamino)-7-oxoheptyl)oxy)-3-(phenylsulfonyl)-1,2,5-oxadiazole 2-oxide (5d)*:* white solid. (Yield: 70%). ^{1}H NMR (600 MHz, DMSO) δ 10.35 (s, 1H), 8.62 (s, 1H), 8.01 (d, *J* =

7.4 Hz, 2H), 7.91 (s, 1H), 7.76 (t, *J* = 7.9 Hz, 2H), 4.38 (t, *J* = 6.3 Hz, 2H), 1.97 (t, *J* = 7.4 Hz, 2H), 1.78 – 1.69 (m, 2H), 1.54 – 1.49 (m, 2H), 1.36 – 1.25 (m, 4H). ^{13}C NMR (151 MHz, d_6-DMSO) δ 169.6, 159.3, 136.6, 130.5, 130.2, 128.7, 127.9, 110.9, 71.9, 32.7, 28.5, 28.2, 25.5, 25.2. HRMS (ESI) m/z calcd for $C_{15}H_{20}N_3O_7S$ $[M+H]^+$ 386.1016, found 386.1032.

4-((8-(hydroxyamino)-8-oxooctyl)oxy)-3-(phenylsulfonyl)-1,2,5-oxadiazole 2-oxide (5e)*:* white solid. (Yield: 64%). ^{1}H NMR (600 MHz, DMSO) δ 10.34 (s, 1H), 8.66 (s, 1H), 8.01 (d, *J* = 7.5 Hz, 2H), 7.91 (t, *J* = 7.4 Hz, 1H), 7.76 (t, *J* = 7.9 Hz, 2H), 4.38 (t, *J* = 6.3 Hz, 2H), 1.96 (t, *J* = 7.3 Hz, 2H), 1.73 (dd, *J* = 13.5, 6.4 Hz, 2H), 1.51 (dt, *J* = 14.5, 7.4 Hz, 2H), 1.35 – 1.21 (m, 6H). ^{13}C NMR (151 MHz, DMSO) δ 169.6, 159.3, 137.8, 136.6, 130.5, 128.7, 110.9, 72.0, 32.7, 28.9, 28.7, 28.3, 25.5, 25.4. HRMS (ESI) m/z calcd for $C_{16}H_{22}N_3O_7S$ $[M+H]^+$ 400.1173, found 400.1172.

4-(2-(2-(hydroxyamino)-2-oxoethoxy)ethoxy)-3-(phenylsulfonyl)-1,2,5-oxadiazole 2-oxide (5f)*:* white solid. (Yield: 66%). M.p. 143-145℃. ^{1}H NMR (600 MHz, d_6-DMSO) δ 10.54 (s, 1H), 8.89 (s, 1H), 8.03 (d, *J* = 7.5 Hz, 2H), 7.90 (t, *J* = 7.5 Hz, 1H), 7.75 (t, *J* = 7.9 Hz, 2H), 4.58 – 4.49 (m, 2H), 3.97 (s, 2H), 3.86 – 3.80 (m, 2H). ^{13}C NMR (400 MHz, d_6-DMSO) δ 171.0, 158.8, 137.2, 136.0, 129.9, 128.2, 110.4, 72.1, 70.6, 68.9, 68.2, 42.8. HRMS (ESI) m/z calcd for $C_{12}H_{14}N_3O_8S$ $[M+H]^+$ 360.0496, found 360.0497.

4-(3-(hydroxyamino)-2,2-dimethyl-3-oxopropoxy)-3-(phenylsulfonyl)-1,2,5-oxadiazole 2-oxide (5g)*:* white solid. (Yield: 71%). M.p. 128-130℃. ^{1}H NMR (600 MHz, d_6-DMSO) δ 10.61 (s,

1H), 8.81 (s, 1H), 7.99 (d, *J* = 7.5 Hz, 2H), 7.90 (t, *J* = 6.8 Hz, 1H), 7.76 (t, *J* = 7.4 Hz, 2H), 4.38 (s, 2H), 1.22 (s, 6H). ^{13}C NMR (400 MHz, d_6-DMSO) δ 171.4, 159.3, 137.9, 136.5, 130.6, 130.6, 128.62, 110.7, 76.99, 41.7, 22.2. HRMS (ESI) m/z calcd for $C_{13}H_{16}N_3O_7S$ $[M+H]^+$ 358.0704, found 358.0703.

(E)-4-((4-(hydroxyamino)-4-oxobut-2-en-1-yl)oxy)-3-(phenylsulfonyl)-1,2,5-oxadiazole 2-oxide (5h)*:* white solid. (Yield: 76%). M.p. 144-146℃. ^{1}H NMR (600 MHz, d_6-DMSO) δ 8.10 (d, *J* = 7.5 Hz, 2H), 7.86 (t, *J* = 7.5 Hz, 1H), 7.73 (t, *J* = 7.9 Hz, 2H), 6.96 (dt, *J* = 15.3, 4.3 Hz, 1H), 6.27 (d, *J* = 15.5 Hz, 1H), 5.15 (d, *J* = 3.1 Hz, 2H). ^{13}C NMR (400 MHz, d_6-DMSO) δ 161.2, 158.6, 139.1, 136.0, 129.9, 128.2, 120.4, 76.7, 69.0. HRMS (ESI) m/z calcd for $C_{12}H_{12}N_3O_7S$ $[M+H]^+$ 342.0390, found 342.0393.

4-(2-(2-(2-(hydroxyamino)-2-oxoethoxy)ethoxy)ethoxy)-3-(phenylsulfonyl)-1,2,5-oxadiazole 2-oxide (5i)*:* white solid. (Yield: 70%). M.p. 139-141℃. ^{1}H NMR (600 MHz, DMSO) δ 10.40 (s, 1H), 8.77 (s, 1H), 8.03 (d, *J* = 7.8 Hz, 2H), 7.91 (t, *J* = 7.4 Hz, 1H), 7.76 (t, *J* = 7.3 Hz, 2H), 4.54 – 4.50 (m, 2H), 3.89 (s, 2H), 3.84 – 3.80 (m, 2H), 3.65 (d, *J* = 3.0 Hz, 2H), 3.61 (d, *J* = 3.2 Hz, 2H). ^{13}C NMR (400 MHz, d_6-DMSO) δ 165.5, 158.8, 137.2, 136.0, 129.9, 128.1, 70.8, 70.2, 69.62, 68.9, 67.7. HRMS (ESI) m/z calcd for $C_{17}H_{14}N_3O_7S$ $[M+H]^+$ 404.0547, found 404.0549.

4-(4-(hydroxycarbamoyl)phenoxy)-3-(phenylsulfonyl)-1,2,5-oxadiazole 2-oxide (5j)*:* white solid. (Yield: 78%). M.p. 171-172℃. ^{1}H NMR (600 MHz, d_6-DMSO) δ 11.29 (s, 1H), 9.10 (s, 1H), 8.04 (d, *J* = 7.3 Hz, 2H), 7.93 (t, *J* = 6.8 Hz, 1H), 7.87 (d, *J* = 7.9 Hz, 2H), 7.77 (t, *J* = 7.4

Hz, 2H), 7.52 (d, *J* = 8.0 Hz, 2H). ^{13}C NMR (400 MHz, d_6-DMSO) δ 163.6, 158.5, 155.1, 137.3, 136.8, 131.4, 130.5, 129.5, 129.1, 119.9, 111.8. HRMS (ESI) m/z calcd for $C_{15}H_{12}N_3O_7S$ $[M+H]^+$ 378.0390, found 378.0439.

4-(3-(hydroxycarbamoyl)phenoxy)-3-(phenylsulfonyl)-1,2,5-oxadiazole 2-oxide (5k): white solid. (Yield: 64%). M.p. 177-179℃. ^{1}H NMR (600 MHz, d_6-DMSO) δ 11.31 (s, 1H), 9.16 (s, 1H), 8.04 (d, *J* = 7.6 Hz, 2H), 7.92 (d, *J* = 7.4 Hz, 1H), 7.78 – 7.72 (m, 4H), 7.62 – 7.57 (m, 2H). ^{13}C NMR (400 MHz, d_6-DMSO) δ 167.3, 157.6, 144.0, 135.4, 129.8, 119.0, 118.9, 117.3, 114.4. HRMS (ESI) m/z calcd for $C_{15}H_{12}N_3O_7S$ $[M+H]^+$ 378.0390, found 378.0378.

4-(4-(hydroxycarbamoyl)-2-methoxyphenoxy)-3-(phenylsulfonyl)-1,2,5-oxadiazole 2-oxide (5l): white solid. (Yield: 72%). M.p. 198-200℃. ^{1}H NMR (600 MHz, d_6-DMSO) δ 11.26 (s, 1H), 9.07 (s, 1H), 8.09 (d, *J* = 7.8 Hz, 2H), 7.95 (t, *J* = 7.4 Hz, 1H), 7.81 (t, *J* = 7.6 Hz, 2H), 7.57 (s, 1H), 7.52 (d, *J* = 8.2 Hz, 1H), 7.44 (d, *J* = 8.5 Hz, 1H), 3.79 (s, 3H). ^{13}C NMR (400 MHz, d_6-DMSO) δ 163.0, 158.4, 149.4, 142.8, 137.0, 136.4, 130.2, 128.4, 121.6, 119.8, 112.1, 110.8, 56.3. HRMS (ESI) m/z calcd for $C_{16}H_{14}N_3O_8S$ $[M+H]^+$ 408.0496, found 408.0500.

4-(4-(2-(hydroxyamino)-2-oxoethyl)phenoxy)-3-(phenylsulfonyl)-1,2,5-oxadiazole 2-oxide (5m): white solid. (Yield: 73%). ^{1}H NMR (600 MHz, d_6-DMSO) δ 10.62 (s, 1H), 8.79 (s, 1H), 8.04 (d, *J* = 7.8 Hz, 2H), 7.92 (t, *J* = 7.4 Hz, 1H), 7.77 (t, *J* = 7.6 Hz, 2H), 7.35 (dd, *J* = 17.3, 8.6 Hz, 4H), 3.34 (s, 2H). ^{13}C NMR (400 MHz, d_6-DMSO) δ 158.3, 136.9, 136.1, 131.3, 130.4,

129.9, 129.5, 128.5, 128.3, 119.3, 29.9.HRMS (ESI) m/z calcd for $C_{16}H_{14}N_3O_7S$ $[M+H]^+$ 392.0547, found 392.0550.

4-((2-(hydroxycarbamoyl)-2-methylpentyl)oxy)-3-(phenylsulfonyl)-1,2,5-oxadiazole 2-oxide (5n)*:* white solid. (Yield: 54%). ^{1}H NMR (600 MHz, DMSO-d_6) δ 10.63 (s, 1H), 8.79 (s, 1H), 8.04 (d, *J* = 7.5 Hz, 2H), 7.92 (t, *J* = 7.5 Hz, 1H), 7.77 (t, *J* = 7.7 Hz, 2H), 7.35 (dd, *J* = 17.9, 8.4 Hz, 4H), 3.34 (s, 2H). ^{13}C NMR (400 MHz, d_6-DMSO) 177.2, 172.4, 131.3, 129.96, 129.5, 128.5, 67.0, 64.9, 47.2, 36.3, 35.7, 19.8, 17.7, 13.7. HRMS (ESI) m/z calcd for $C_{15}H_{20}N_3O_7S$ $[M+H]^+$ 386.1016, found 386.1017.

(E)-4-(4-(3-(hydroxyamino)-3-oxoprop-1-en-1-yl)phenoxy)-3-(phenylsulfonyl)-1,2,5-oxadiazole 2-oxide (5o)*:* white solid. (Yield: 69%). M.p. 153-155℃. ^{1}H NMR (600 MHz, DMSO) δ 10.79 (s, 1H), 9.08 (s, 1H), 7.91 (d, *J* = 8.5 Hz, 1H), 7.76 (dd, *J* = 25.3, 7.9 Hz, 2H), 7.63 (d, *J* = 8.4 Hz, 2H), 7.47 (d, *J* = 15.9 Hz, 1H), 7.34 (dd, *J* = 15.9, 8.4 Hz, 2H), 7.29 (d, *J* = 8.5 Hz, 2H), 6.44 (d, *J* = 15.8 Hz, 1H).^{13}C NMR (400 MHz, d_6-DMSO) δ 163.3, 158.7, 138.3, 129.0, 125.8, 115.6, 115.4. HRMS (ESI) m/z calcd for $C_{14}H_{18}N_3O_9S$ $[M+H]^+$ 404.0758, found 404.0755.

In Vitro Hela Extracts Inhibition Fluorescence Assay.

In vitro HDACs inhibition assays were conducted as previously described in our group.[31] In brief, 10 μL of HELA extracts were mixed with various concentrations of 50 μL tested compounds (0.039, 0.39, 1.56, 6.25, 25, 100 μM) and SAHA as the positive control. Five minutes later, fluorogenic substrate Boc-Lys (acetyl)-AMC (40 μL) was added, and the mixture

was incubated at 37℃ for 30 minutes and then stopped by addition of 100 μL of developer containing trypsin and TSA. After incubation at 37℃ for 20 minutes, fluorescence intensity was measured using a microplate reader at excitation and emission wavelengths of 390 nm and 460 nm, respectively. The inhibition ratios were calculated from the fluorescence intensity readings of tested wells relative to those of control wells, and the IC_{50} values were calculated using a regression analysis of the concentration/inhibition data.

In Vitro Antiproliferative Assay.

In vitro antiproliferative assays were determined by the MTT (3-(4,5-dimethylthiazol-2-yl)-2,5-diphenyltetrazolium bromide) method as previously described.[31] Briefly, all cell lines were maintained in RPMI1640 medium containing 10% FBS at 37℃ in 5% CO_2 humidified incubator. Cells were passaged the day before dosing into a 96-well cell plate and allowed to grow for a minimum of 4h prior to addition of compounds. After compounds addition, the plates were incubated for an additional 48h, and then 0.5% MTT solution was added to each well. After further incubation for 4h, formazan formed from MTT was extracted by adding 200 μL of DMSO for 15 min. Absorbance was then determined using an ELISA reader at 490 nm and 630 nm, and the IC_{50} values were calculated according to the inhibition ratios.

In Vitro Nitrite Measurement.

The nitrite measurement in vitro was tested using the reported method.[33] The levels of NO

generated by individual compounds in the cells are presented as that of nitrite and were determined by the colorimetric assay using the colorimetric assay kit (purchased from Beyotime, China), according to the manufacturer's instruction. Briefly, HEL cells (5×10^5/well) were treated with a 100 μM of tested compounds for 3h or 5h. Subsequently, the cells were harvested, and their cell lysates were prepared and then mixed with Griess for 10 min at 37℃, followed by measurement at 540 nm by an enzyme-linked immunosorbent assay plate reader. The cells treated with DMSO were used as negative controls for the background levels of nitrite production, while sodium nitrite at different concentrations was prepared as the positive control for the standard curve.

In Vitro Antiproliferative Assay with Hemoglobin.

This assay was determined by the MTT (3-(4,5-dimethylthiazol-2-yl)-2,5-diphenyltetrazolium bromide) method as previously described in vitro antiproliferative assay. Briefly, HEL cell lines were maintained in RPMI1640 medium containing 10% FBS at 37℃ in 5% CO_2 humidified incubator. Cells were passaged the day before dosing into a 96-well cell plate and allowed to grow for a minimum of 4h prior to addition of hemoglobin and **5c**. HEL cells were pretreated with the indicated concentrations of NO scavenger hemoglobin (0, 2.5, 5, 10 and 20 μM) for 1 hour and treated 2 μM **5c** for 24 hours. After compounds addition, the plates were incubated for an additional 48 h, and then 0.5% MTT solution was added to each well. After further incubation for 4 h, formazan formed from MTT was extracted by adding 200 μL of DMSO for 15 min. Absorbance was then determined using an ELISA reader at 490 nm and 630

nm, and the IC_{50} values were calculated according to the inhibition rations.

In Vitro Cell Apoptosis Assay.

HEL (1×10^5/well) cells were incubated in six-well plates for 24h, and then treated with 0.1% DMSO (as control), various doses of SAHA, **5c** (0.5, 1, 2 μM) in fresh growth medium. After 24 h, the growth medium was collected, and the cells were trypsined and collected with the corresponding medium. After centrifugation at 2000 r/min at 4℃ for 5 min, the supernatant was removed completely, and the cells were washed twice with pre-chilled PBS. A 200 μL volume of 1× binding buffer, 2.5 μL of 7-AAD, and 2.5 μL of propidium iodide were added (PE-Annexin V kit, BD pharmingen). The cells were gently vortex-mixed and incubated for 15min at 25℃ in the dark. Using cells stained with 7-AAD and propidium iodide alone as the positive control, the samples were detected and performed with an FACS Calibur flow cytometer (Becton Dickinson).

In Vitro Cell Cycle Assay.

HEL cells were seeded into six-well plates at a density of 4×10^5 per well. After overnight incubation, cells were treated with the same concentration (0.5 μM) of **5c**, **2** and SAHA. After 48h treatment, cells were harvested and fixed with 70% ethanol phosphate buffer overnight. Then the cells were washed with PBS twice, incubated with DNase-free RNase A (1 mg/mL, Solarbio, China) for 30 min, and stained with propidium iodide (50 mg/mL, Solarbio, China) for 30 min, avoiding light at room temperature. DNA content was measured by a fluorescence-activated cell cytometer (FACScan, Becton Dickinson, USA) and analyzed by

MODFit LT for Mac V3.0 software.

In Vivo Antitumor Assay against HEL.

In vivo human tumor xenograft models were established as previously described in our lab.[31] In brief, HEL tumor cell lines was cultured in RPMI1640 medium containing 10% FBS and maintained in a 5% CO_2 humidified incubator at 37℃. For in vivo antitumor assays, aforementioned cells were inoculated subcutaneously in the right flanks of male athymic nude mice (BALB/c-nu, 6-8 weeks old, HFK Bioscience Co., LTD, Beijing, China). About 10 days after injection, tumors were palpable (about 100 mm^3) and mice were randomized into treatment and control groups (6 mice per group). The treatment groups received the compound **5c** (120 mg/Kg/day, 100 mg/Kg/day) and SAHA (120 mg/Kg/day) by oral administration, and the blank control group received an equal volume of PBS solution containing DMSO. During treatment, subcutaneous tumors were measured with a vernier caliper every three days, and body weight was monitored regularly. After treatment, mice were sacrificed and dissected to weigh the tumor tissues and to examine the internal organ injury. Tumor growth inhibition (TGI) and relative increment ratio (T/C) were calculated as described in our lab group[31] at the end of treatment to reveal the antitumor effects in tumor weight and tumor volume, respectively.

$$\mathrm{TGI} = \frac{\text{the mean tumor weight of control group} - \text{the mean tumor weight of treated}}{\text{the mean tumor weight of control group}} \times 100\%$$

Tumor volume (V) was estimated using the equation ($V = ab^2/2$, where a and b stand for the

longest and shortest diameter, respectively). T/C was calculated according to the following formula:

$$\frac{T}{C} = \frac{\text{the mean RTV of treated group}}{\text{the mean RTV of control group}}$$

RTV, namely relative tumor volume =V_t/V_0, (V_t: the tumor volume measured at the end of treatment; V_0: the tumor volume measured at the beginning of treatment). All the obtained data were used to evaluate the antitumor potency and toxicity of compounds. Data were analyzed by Student's two-tailed *t* test. A P level <0.05 was considered statistically significant.

In Vitro HDACs Isoform Selectivity Fluorescence Assay.

This assay was conducted by Shanghai Huawei pharmaceutical Co. Ltd., China. The HDAC1, HDAC6 enzymes were purchased from Abcam (#AB101661, #AB42632). The HDAC2, HDAC3, HDAC4, HDAC8, HDAC11 enzyme were purchased from SignalChem (#H84-30G, #H85-30G, #H86-31G, #H90-30H, #H93-30G). All of the enzymatic reactions were conducted at 37℃for 30 minutes. The 50 μL reaction mixture contains 25 mM Tris, pH 8.0, 1 mM $MgCl_2$, 0.1 mg/ml BSA, 137 mM NaCl, 2.7 mM KCl, HDAC and the corresponding enzyme substrate (the enzyme substrate of HDAC 1, 2, 3 and 6 is Ac-Leu-GlyLys(Ac)-AMC; the enzyme substrate of HDAC 4, 5, 7, 8 and 9 is Ac-Leu-Gly-Lys(Tfa)-AMC; the enzyme substrate of HDAC 10 is Ac-Arg-His-Lys(Ac)-Lys(Ac)-AMC). The compounds were diluted in 10% DMSO and 5 μL of the dilution was added to a 50 μL reaction so that the final concentration of DMSO is 1% in all of reactions. The assay was performed by quantitating the fluorescent

product amount of in solution following a enzyme reaction. Fluorescence is then analyzed with an excitation of 350-360 nm and an emission wavelength of 450-460 nm at SpectraMax M5 microtiter plate reader. The IC_{50} values were calculated using nonlinear regression with normalized dose-response fit using Prism GraphPad sofeware.

Western Blotting Analysis.

MV4-11 AML cells (1×10^6/well) or HEL (1×10^6/well) cells were incubated in six-well plates for overnight, and then treated with DMSO (as solvent control), the different concentration 0.1, 1.0 and 10 μM of **5c**. After 3h, the cells were harvested and washed with PBS (0.1 M, pH 7.4), centrifuged, and resuspended in cell lysis solution containing 20 mM Tris (pH 7.5), 150 mM NaCl, 1% Triton X-100 and several protein inhibitors such as sodium pyrophosphate, b-glyc erophosphate, EDTA, Na_3PO_4 and leupeptin (Beyotime Biotech., China) for 30 min, then centrifuged for 15 min at 12 000 rpm at 4 ℃, and the supernatant was the whole-cell extracts. Total proteinextracts (20 μg per lane) were separated by 10% SDS polyacrylamide gel electrophoresis and transferred onto PVDF membranes (Cat. IPVH00010, Millipore). Membrane was blocked with 5% S36 milk in TBS-T (10 mM Tris [pH 7.4], 150 mM NaCl, and 0.1% Tween 20) for 1h at room temperature, then incubated with a 1:1000 dilution of primary antibody overnight at 4 ℃. Then the membrane was washed 10 min ($\times$3) and incubated at 1:2000 dilution of antirabbit goat-HRP-conjugated secondary antibodies for 1.5h at room temperature. Finally the membrane was washed another 10 min ($\times$3) and developed by enhanced chemiluminescence (ECL, Cat. WBKLS0050, Millipore).

■ ASSOCIATED CONTENT

Supporting Information. ^{1}H NMR, ^{13}C NMR spectrum of all targets compounds and HPLC analysis chromatograms of representative target compounds **5a**, **5b**, **5c**, **5j**. This material is available free of charge via the Internet at http://pubs.acs.org.

■ AUTHOR INFORMATION

Corresponding Author

*(W.X.) Phone: 86-531-88382264. Fax: 86-531-88382264. E-mail: wenfxu@gmail.com.

*(Y.Z.) Phone: 86-531-88382009. Fax: 86-531-88382009. E-mail: zhangyingjie@sdu.edu.cn.

■ ACKNOWLEDGMENT

This work was supported by National High-tech R&D Program of China, 863 Program (Grant No.2014AA020523), National Natural Science Foundation of China (Grant no. 21302111, Grant no. 81373282 and Grant no. 21172134), China Postdoctoral Science Foundation funded project (Grant no. 2013M540558, Grant no.2014T70654), and National Cancer Institute of the National Institutes of Health (Award no. R01CA163452)

■ ABBREVIATIONS:

HDAC, histone deacetylase; HDACI, histone deacetylase inhibitor; SAHA, suberoylanilide hydroxamic acid; NO, nitrate oxide; EtOAc, acetic ether; TEA, triethylamine; PCC, Pyridinium Chlorochromate; DCM, dichloromethane; Py, pyridine.

■ REFERENCES

(1) Muller. S.; H. Kramer. O. Inhibitors of HDACs - Effective Drugs against Cancer. *Current Cancer Drug Targets*, **2010**, *10*, 210-228.

(2) B. Venugopal; T. R. J. Evans. Developing Histone Deactylase Inhibitors as Anti-Cancer Therapeutics. *Current Medicinal Chemistry*, **2011**, *18*, 1658-1671.

(3) Marielle Paris; Marina Porcelloni; Monica Binaschi; Daniela Fattori. Histone Deacetylase Inhibitors: from Bench to Clinic. *J. Med. Chem.* **2008**, *51*, 1505-1529.

(4) Bertrand, P. Inside HDAC with HDAC inhibitors. *Eur. J. Med. Chem.* **2010**, *45*, 2095−2116.

(5) Li, ZhM; Zhu, WG. Targeting Histone Deacetylases for Cancer Therapy: from Molecular Mechanisms to Clinical Implications. *Int. J. Biol. Sci.* **2014**, *7*, 757-770.

(6) Marks, P. A. Discovery and Development of SAHA as an Anticancer Agent. *Oncogene.* **2007**, *26*, 1351–1356.

(7) Marks, P. A.; Breslow, R. Dimethyl Sulfoxide to Vorinostat: Development of this Histone Deacetylase Inhibitor as an Anticancer Drug. *Nat. Biotechnol.* **2007**, *25*, 84–90.

(8) Varasi M., Thaler F., Abate A., Bigogno C., Boggio R., Carenzi G., Cataudella T., Zuffo R. D., Fulco M. C., Rozio M. G., Mai A., Dondio G., Minucci S., and Mercurio C. Discovery, Synthesis, and Pharmacological Evaluation of Spiropiperidine Hydroxamic Acid Based Derivatives as Structurally Novel Histone Deacetylase (HDAC) Inhibitors. *J. Med. Chem.* **2011**, *54*, 3051–3064

(9) Scatena R ,Bottoni P ,Martorana GE , et al . Nitric Oxide Donor Drugs: an Update on Pathophysiology and Threapreutically Potential. *Exert. Opin. Investg. Drug.* **2005**, *14*, 835 – 846.

(10) Megson I. L. Nitric Oxide Donor Drugs. *Drugs Fut,* **2000**, *25*, 701-705.

(11) Nathan C.F., Hibbs J.B., Jr. Role of Nitric Oxide Synthesis in Macrophage Antimicrobial Activity. *Curr. Opin. Immunol.* **1991**, *3*, 65-70

(12) Stuehr D.J., Nathan C.F. Nitric oxide. A Macrophage Product Responsible for Cytostasis and Respiratory Inhibition in Tumor Target Cells. *J. Exp. Med.* **1989**, *169*, 1543-1555

(13) Bonfoco E, Krainc D, Ankarcrona M. Apoptosis and Necrosis: Two Distinct Events Induced, Respectively, by Mild and Intense Insults with N-methyl-D-aspartate or Nitric Oxide/Superoxide in Cortical Cell Cultures. *Proc. Natl. Acad. Sci*, **1995**, *92*: 7162-7166

(14) Konovalova NP, Goncharova SA, Volkova LM, et al. Nitric Oxide Donor Increase the Efficiency of Cytostatic Therapy and Retards the Development of Drug Resistance. *Nitric Oxide*, **2003**, *8*: 59-64

(15) Wang PG, Xian M, Tang XP, et al. Nitric Oxide Donors: Chemical Activities and Biological Applications. *Chem. Rev.* **2002**, *102*: 1091-1134

(16) Dhar, A.; Brindley, J. M.; Stark, C.; Citro, M. L.; Keefer, L. K.; Colburn, N. H. Nitric Oxide does not Mediate but Inhibits Transformation and Tumor Phenotype. *Mol. Cancer. Ther.* **2003**, *2*, 1285-1293.

(17) Maksimovic-Ivanic, D.; Mijatovic, S.; Harhaji, L.; Miljkovic, D.; Dabideen, D.; Fan Cheng, K.; Mangano, K.; Malaponte, G.; Al-Abed, Y.; Libra, M.; Garotta, G.; Nicoletti, F.; Stosic-Grujicic, S. Anticancer Properties of the Novel Nitric Oxide-Donating Compound (S,R)-3-phenyl-4,5-dihydro-5-isoxazole Acetic Acid-Nitric Oxide in Vitro and in Vivo. *Mol. Cancer Ther.* **2008**, *7*, 510-520.

(18) Feelisch M，Schonafinger K，Noack E． Thiol-mediated Generation of Nitric Oxide accounts for the Vasodilator Action of Phenylsulfonylfuroxans. *Biochem Pharmacol*. **1992**, *44*, 1149-1157.

(19) Chen, L.; Zhang, Y.; Kong, X.; Lan, E.; Huang, Z.; Peng, S.; Kaufman, D. L.; Tian, J. Design, Synthesis, and Antihepatocellular Carcinoma Activity of Nitric Oxide Releasing Derivatives of Oleanolic Acid. *J. Med. Chem.* **2008**, *51*, 4834-4838.

(20) Ling, Y.; Ye, X. L.; Ji, H.; Zhang, Y. H.; Lai, Y. Sh.; Peng, S. X.; Tian, J. D. Synthesis and Evaluation of Nitric Oxide-Releasing Derivatives of Farnesylthiosalicylic Acid as Anti-Tumor

Agents. *Bioorg. Med. Chem.* **2010**, *18*, 3448-3456.

(21) Moharram, S.; Zhou, A.; Wiebe, L. I.; Knaus, E. E. Design and Synthesis of 3‘- and 5‘-O-(3-Benzenesulfonylphenylsulfonylfuroxan-4-yl)-2‘-deoxyuridines: Biological Evaluation as Hybrid Nitric Oxide Donor−Nucleoside Anticancer Agents. *J. Med. Chem.* **2004**, *47*, 1840-1846.

(22) Han, Ch.; Huang, Zh. J.; Zheng, Ch.; Wan, L. D.; Zhang, L. W.; Peng, S. X.; Ding, K.; Ji, H. B.; Tian, J. D.; Zhang, Y. H. Novel Hybrids of Phenylsulfonylfuroxan and Anilinopyrimidine as Potent and Selective Epidermal Growth Factor Receptor Inhibitors for Intervention of Non-Small-Cell Lung Cancer. *J. Med. Chem.* **2013**, *56*, 4738−4748.

(23) Illi, B.; Dello Russo, C.; Colussi, C.; Rosati, J.; Pallaoro, M.; Spallotta, F.; Rotili, D.; Valente, S.; Ragone, G.; Martelli, F.; Biglioli, P.; Steinkuhler, C.; Gallinari, P.; Mai, A.; Capogrossi, M. C.; Gaetano, C. Nitric Oxide Modulates Chromatin folding in Human Endothelial Cells via Protein Phosphatase 2A Activation and Class II Histone Deacetylases Nuclear Shuttling. *Circ. Res.* **2008**, *102*, 51−58.

(24) Colussi, C.; Mozzetta, C.; Gurtner, A.; Illi, B.; Rosati, J.; Straino, S.; Ragone, G.; Pescatori, M.; Zaccagnini, G.; Antonini, A.; Minetti, G.; Martelli, F.; Piaggio, G.; Gallinari, P.; Steinkulher, C.; Clementi, E.; Dell’Aversana, C.; Altucci, L.; Mai, A.; Capogrossi, M. C.; Puri, P. L.; Gaetano, C. HDAC2 Blockade by Nitric Oxide and Histone Deacetylase Inhibitors Reveals a Common Target in Duchenne Muscular Dystrophy Treatment. *Proc. Natl. Acad. Sci. U.S.A.* **2008**, *105*,

19183−19187.

(25) Feng, J.H; Jing F.B; Fang, H; Gu L.Ch; Xu W.F. Expression, Purification, and S-nitrosylation of Recombinant Histone Deacetylase 8 in Escherichia Coli. *BioScience Trends*. **2011**, *5*: 17-22

(26) Alexi Nott, P. Marc Watson, James D. Robinson, Luca Crepaldi and Antonella Riccio. S-nitrosylation of Histone Deacetylase 2 Induces Chromatin Remodeling in Neurons. *Nature*. **2008**, *455*, 411-415

(27) Spallotta, F.; Cencioni, C.; Straino, S.; Nanni, S.; Rosati, J.; Artuso, S.; Manni, I.; Colussi, C.; Piaggio, G.; Martelli, F.; Valente, S.; Mai, A.; Capogrossi, M. C.; Farsetti, A.; Gaetano, C. A Nitric Oxide-Dependent Cross-Talk between Class I and III Histone Deacetylases Accelerates Skin Repair. *J. Biol. Chem.* **2013**, *288*, 11004−11012.

(28) Kee, H. J.; Kook, H. Roles and Targets of Class I and IIa Histone Deacetylases in Cardiac Hypertrophy. *J. Biomed. Biotechnol.* **2011**, 928326.

(29) Isenberg, J. S.; Ridnour, L. A.; Espey, M. G.; Wink, D. A.; Roberts, D. D. Nitric Oxide in Wound-Healing. *Microsurgery*, **2005**, *25*, 442−451.

(30) Soneja, A.; Drews, M.; Malinski, T. Role of Nitric Oxide, Nitroxidative and Oxidative stress in Wound Healing. *Pharmacol. Rep.* **2005**, *57*, 108−119.

(31) Zhang, YJ; Fang, H.; Feng, JH.; Jia, YP.; Wang, XJ.; Xu, WF. Discovery of a Tetrahydroisoquinoline-Based Hydroxamic Acid Derivative (ZYJ-34c) as Histone Deacetylase Inhibitor with Potent Oral Antitumor Activities. *J. Med. Chem.* **2011**, *54*, 5532–5539

(32) Ling, Y.; Ye, X. L.; Zhang, ZhZh.; Zhang, Y. H.; Lai, Y. Sh.;Ji, H.; Peng, S. X.; Tian, J. D. Novel Nitric Oxide-Releasing Derivatives of Farnesylthiosalicylic Acid: Synthesis and Evaluation of Antihepatocellular Carcinoma Activity. *J. Med. Chem.* **2011**, *54*, 3251–3259.

(33) Emily Borretto, Loretta Lazzarato, Francesco Spallotta, Chiara Cencioni, Yuri D'Alessandra, Carlo Gaetano, Roberta Fruttero, Alberto Gasco. Synthesis and Biological Evaluation of the First Example of NO Donor Histone Deacetylase Inhibitor. *ACS Med. Chem. Lett.* **2013**, *4*, 994−999.

Table 1. The HELA extract inhibitory activities of compounds.

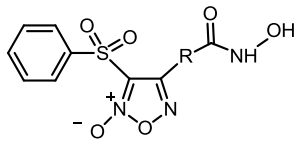

Compd	R	IC_{50}[a] of HELA extract (μM)	Compd	R	IC_{50}[a] of HELA extract (μM)
5a	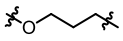	0.047±0.011	**5j**	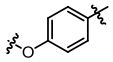	0.047±0.004
5b	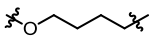	0.13±0.05	**5k**	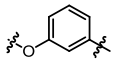	1.6±0.2
5c	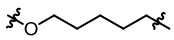	0.038±0.012	**5l**	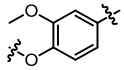	7.3±0.7
5d	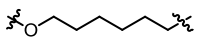	0.054±0.005	**5m**	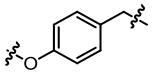	0.14±0.02
5e	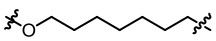	0.063±0.004	**5n**	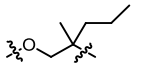	>10^3
5f	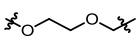	1.5±0.1	**5o**	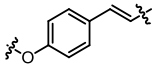	0.15±0.04
5g	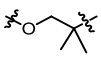	>10^3	**3c**	----	>10^3
5h	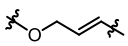	3.7±1.6	**2**	----	>10^3
5i	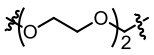	4.3±1.8	SAHA	----	0.11±0.02

a. Results expressed as the mean ± standard deviation of at least three separate determinations.

Table 2. The structure and inhibitory activities of compounds **5a**~**5o**, **3c**, **2** and SAHA against several tumor **cell lines.**

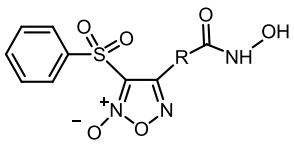

Compd	R	IC_{50}[a] (μM)							
		HEL	HCT-116	Hela	U937	3-AO	MDA	ES-2	KG1
5a	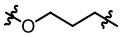	0.67±0.28	3.83±0.74	4.79±3.4	3.30±0.76	21.99±5.33	6.20±1.13	3.78±0.02	1.48±0.03
5b	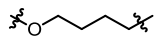	1.03±0.02	2.18±0.14	3.65±0.76	2.91±1.09	4.30±0.20	2.53±0.70	2.53±0.40	1.91±0.03
5c	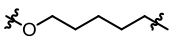	0.38±0.01	1.51±0.29	1.55±0.01	3.10±0.64	5.84±0.27	2.25±0.11	1.39±0.32	1.75±0.19
5d	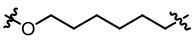	9.33±0.13	4.69±0.81	4.09±0.89	9.93±0.78	ND[b]	1.21±0.97	7.73±0.04	4.27±0.04
5e	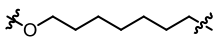	10.77±1.48	2.61±0.68	5.03±0.65	9.30±1.72	ND	2.7±0.43	1.32±0.12	0.63±0.09
5f	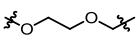	6.79±0.76	13.40±2.32	6.69±0.31	8.15±1.40	19.8±0.29	15.10±3.16	8.69±0.23	7.40±0.97
5g	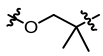	5.01±0.12	9.74±0.27	6.36±0.00	12.52±3.05	18.33±1.93	9.55±0.38	6.88±2.12	6.08±0.76
5h	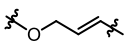	ND	59.92±11.75	8.74±1.33	48.00±2.25	57.70±0.00	47.71±3.48	19.09±0.01	ND
5i	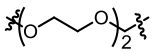	3.73±0.17	11.69±4.14	5.14±0.42	12.13±2.37	19.4±0.02	15.76±1.53	18.11±0.27	5.38±2.39
5j	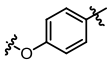	0.92±0.62	2.70±0.41	1.73±0.48	4.73±0.41	4.35±0.07	6.66±1.59	2.19±0.01	1.24±0.08
5k	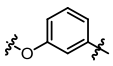	2.60±0.81	4.57±0.77	4.67±0.66	6.49±1.44	9.94±0.19	13.94±3.02	4.19±0.03	1.86±0.06
5l	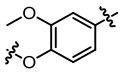	5.55±0.53	5.03±0.17	2.26±0.39	3.64±1.44	1.24±0.11	8.02±0.70	3.55±0.29	1.65±1.25
5m	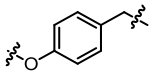	12.99±3.85	14.19±8.01	10.43±1.84	5.01±1.32	22.25±2.20	15.02±2.61	4.13±0.27	1.80±0.37
5n	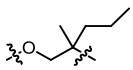	71.46±14.3	66.10±11.9	ND	25.42±16.37	88.66±4.12	60.45±19.99	93.3±2.66	4.06±0.21
5o	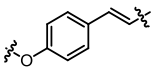	2.41±0.06	8.09±5.32	10.44±1.34	16.10±4.53	38.08±0.00	25.60±6.23	24.05±5.96	2.75±0.30
3c	----	2.16±0.14	ND	ND	ND	ND	ND	ND	ND
2	----	0.69±0.02	ND	ND	ND	ND	ND	ND	ND
SAHA	----	2.42±0.46	4.25±0.59	12.28±0.74	5.49±1.21	3.46±0.23	6.55±1.25	3.22±0.07	0.68±0.35

SAHA+**2**	----	0.53±0.06 [c]	ND	ND	ND	ND	ND	ND	ND

[a] Results expressed as the mean ± standard deviation of at least three separate determinations.

[b] Not Determined

[c] This data means that 0.53 μM SAHA plus 0.53 μM compound **2**.

Table 3. In Vivo antitumor activity in the HEL xenograft model [a]

Compd	TGI (%)	*T/C* (%)
SAHA (120 mg/kg/day)	39	46
5c (120 mg/kg/day)	48	39
5c (100 mg/kg/day)	38	56

[a] Compared with the control group, all treated groups showed statistically significant ($P < 0.05$) T/C and TGI by Student's two-tailed *t* test.

Table 4. The HDACs inhibitory activities of compound **5c**.

Compd	IC_{50}[a] (nM)						
	HDAC 1	HDAC 2	HDAC 3	HDAC 4	HDAC 6	HDAC 8	HDAC 11
SAHA	38.0±2.8	120.5±0.7	58.5±6.4	>100	21.5±0.7	5.5±0.8	34.5±3.5
5c	241.0±12.7	380.5±42.4	532.0±4.2	30.0±10.5	7.4±0.1	343.0±41.0	608.0±87.7

a. Results expressed as the mean ± standard deviation of at least three separate determinations.

Figure legends

Figure 1. Pharmacophore model and structures of representative HDACi.

Figure 2. The chemical structure of Oxadiazole and Phenylsulfonylfuroxan.

Figure 3. The chemical structure of MS275 and NO-MS275.

Figure 4. Design strategy of the target compounds.

Figure 5. NO production by indicated compounds and SAHA in HEL cell. Data are the mean value ± SD obtained from threeindependent experiments.

Figure 6. Effects of hemoglobin on the antiliferative of **5c** in HEL. Data are the mean value ± SD obtained from three independent experiments.

Figure 7. Apoptotic index analysis of SAHA, **2** and **5c** in different concentration in HEL cells.

Figure 8. Effect of SAHA, **2** and **5c** in HEL cells cycle progression.

Figure 9. Growth curve of implanted HEL xenograft in nude mice. Data are expressed as the mean ± standard deviation.

Figure 10. Picture of dissected HEL tumor tissues.

Figure 11. Growth curve of nude mouse weight. Data are expressed as the mean ± standard deviation.

Figure12. (A)Western blot analysis of acetylated tubulin, tubulin, acetylated histone H3, acetylated histone H4 and histone H3 after 3 h treatment with 12.5, 25, 50, 100 and 200 nM **5c** in MV4-11 AML cells. (B) Western blot analysis of HDAC2 after 3 h treatment with 0.1, 1 and 10 μM **5c** in HEL cells. (C) Western blot analysis of HDAC2 after 5 h treatment with 10 μM **5c** and 20, 100, 300 μM PTIO in HEL cells.

Figure 1.

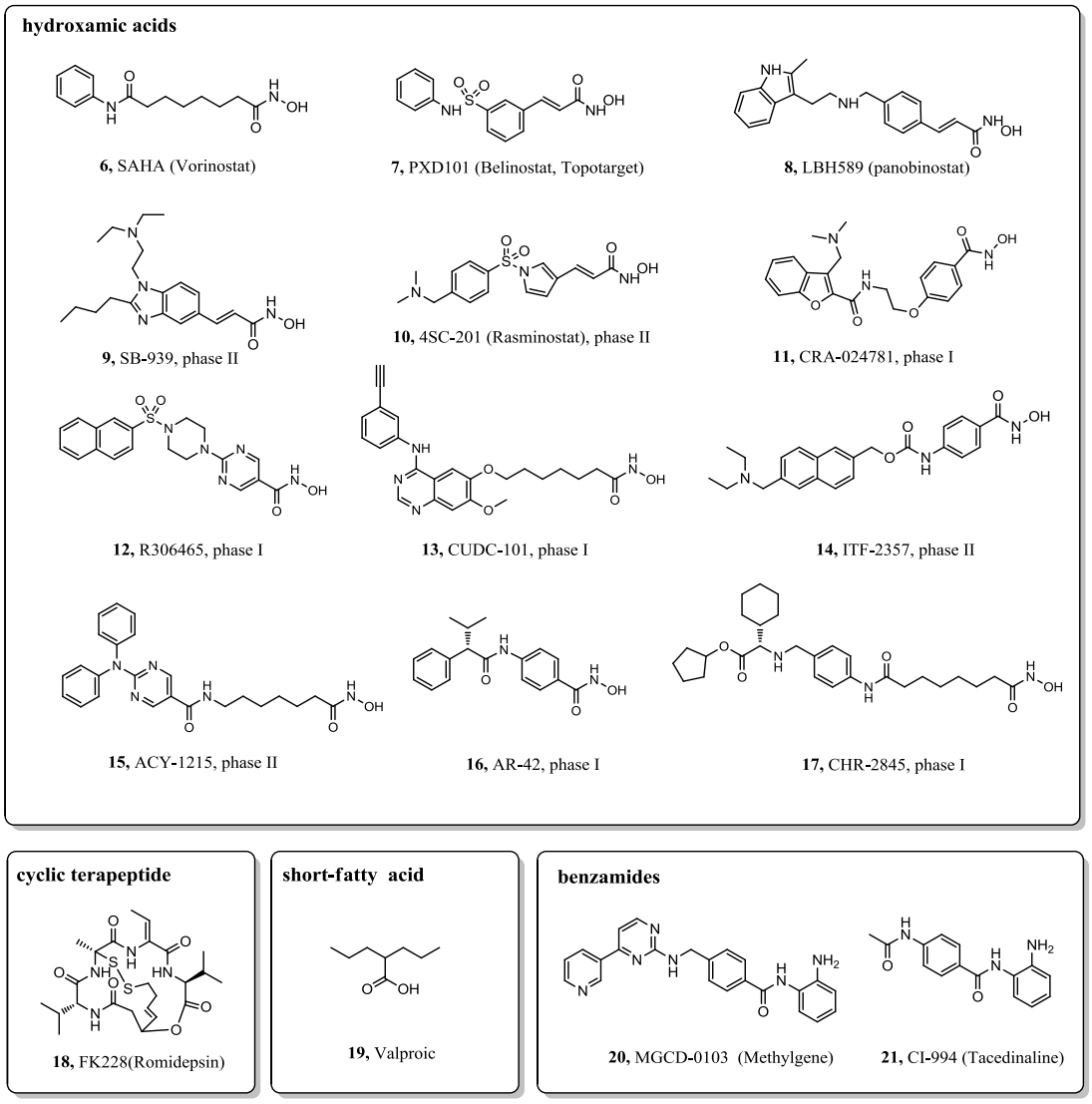

Figure 2.

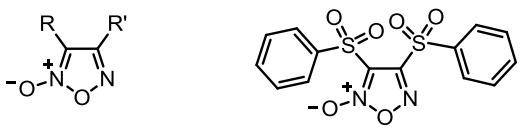

Figure 3.

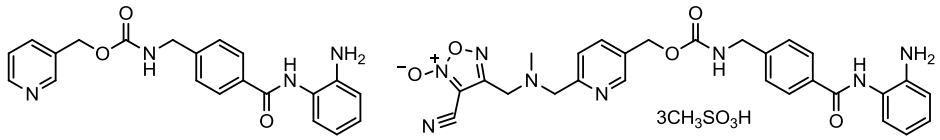

24, MS275 **25**, NO-MS275

Figure 4.

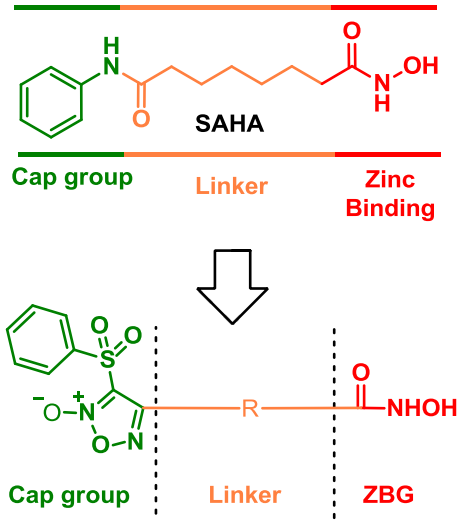

Figure 5.

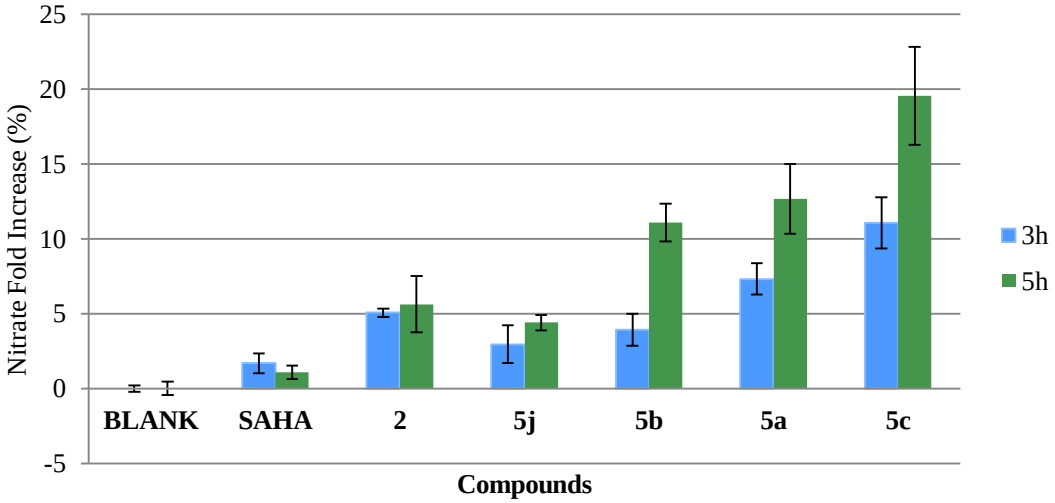

Figure 6.

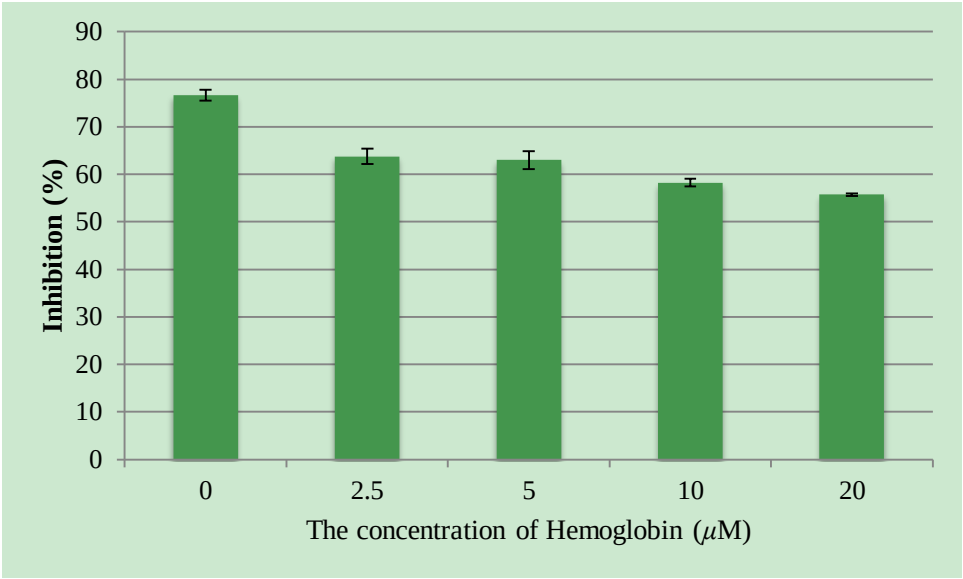

Figure 7.

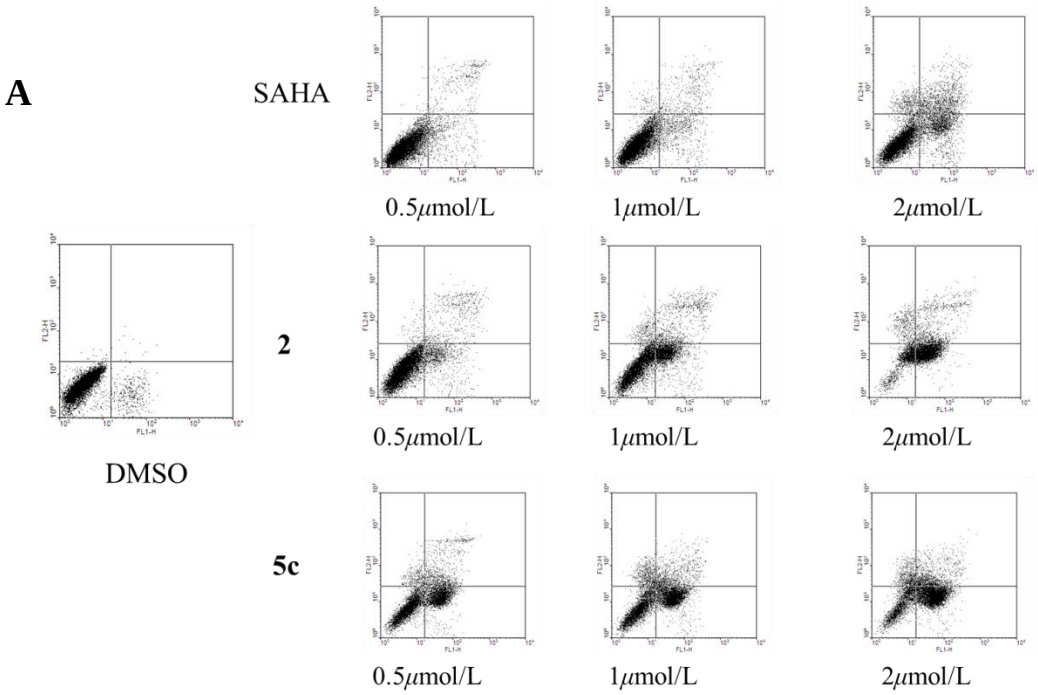

B

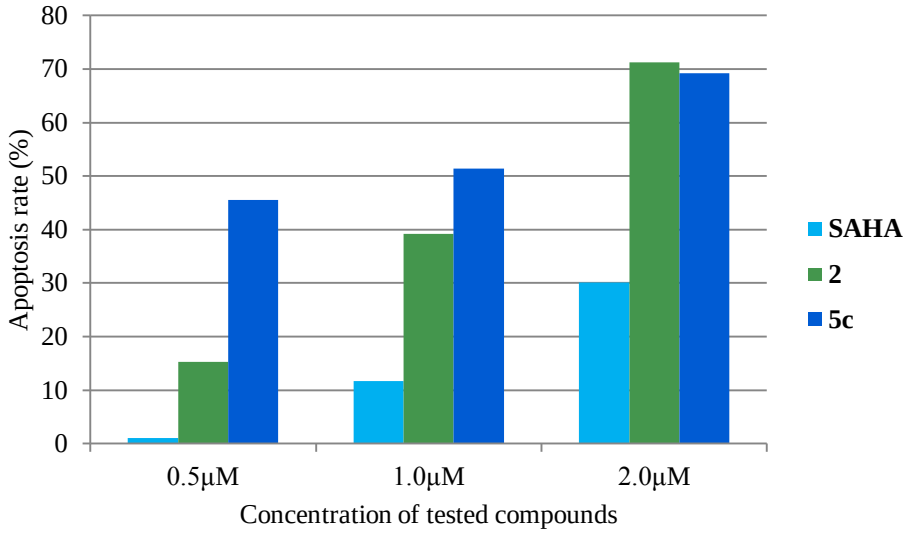
80
70
60
50
40
30
20
10
0
Apoptosis rate (%)
0.5μM
1.0μM
2.0μM
Concentration of tested compounds
SAHA
2
5c

Figure 8.

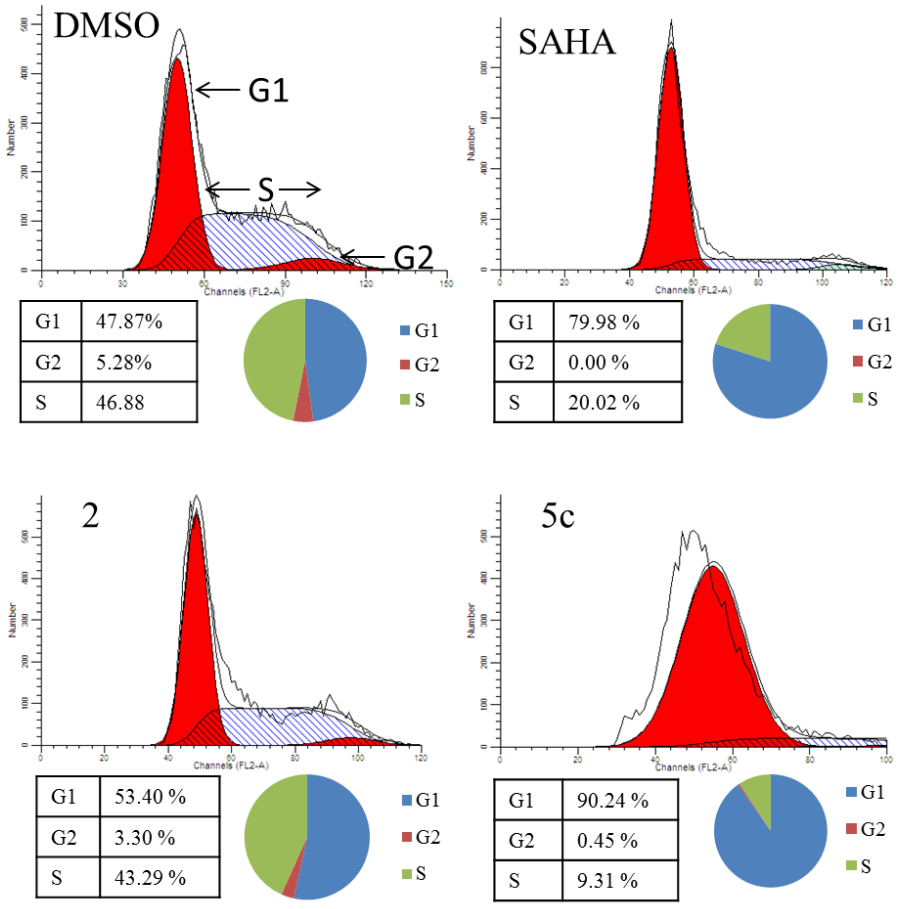
DMSO
G1
S
G2
Number
Channels (FL2-A)
G1 47.87%
G2 5.28%
S 46.88
SAHA
G1 79.98 %
G2 0.00 %
S 20.02 %
2
G1 53.40 %
G2 3.30 %
S 43.29 %
5c
G1 90.24 %
G2 0.45 %
S 9.31 %

Figure 9.

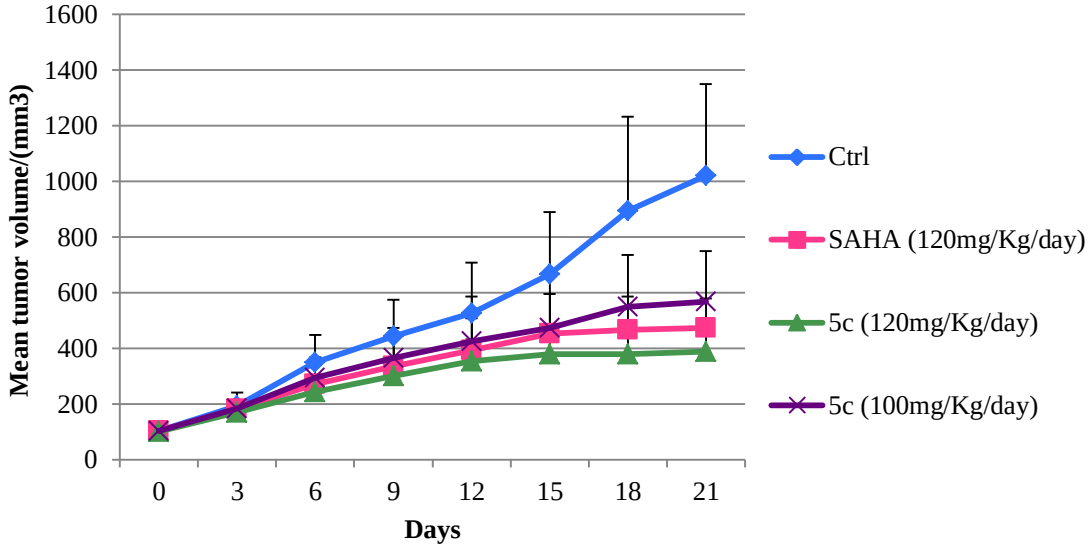

Figure 10.

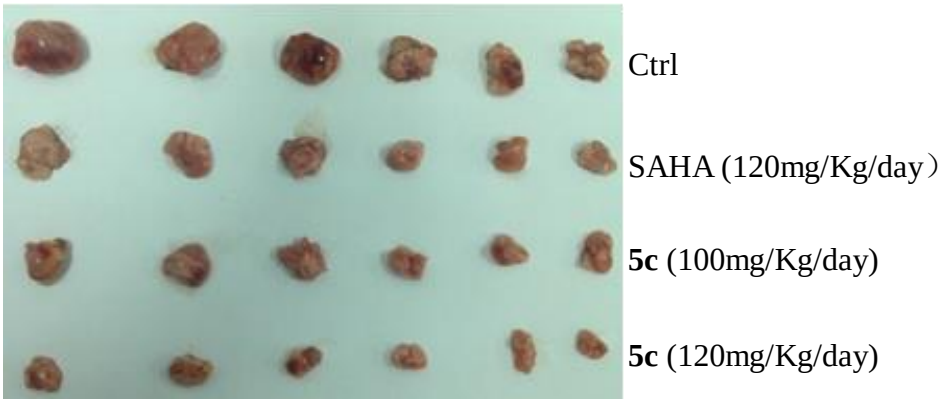

Figure 11.

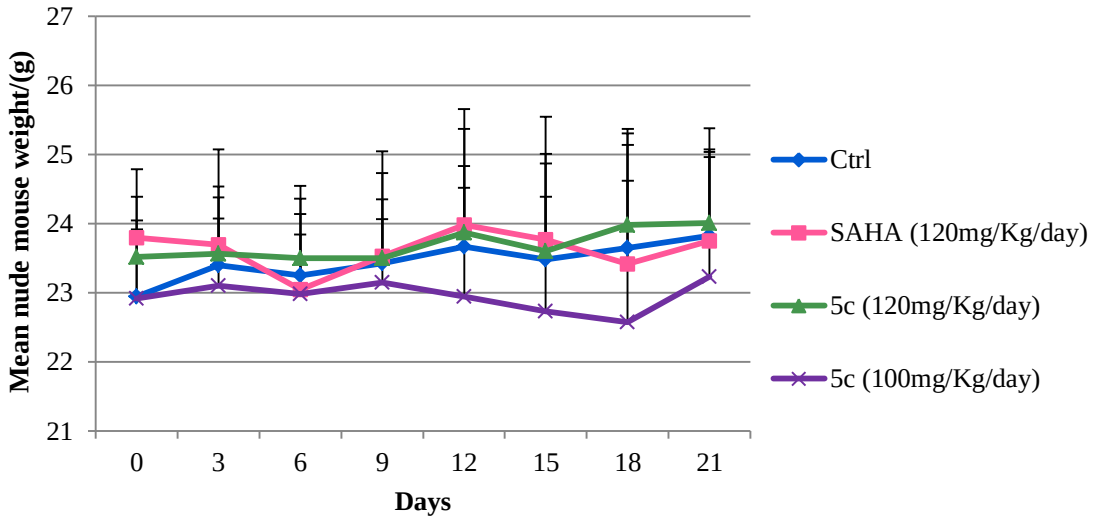

Figure12.

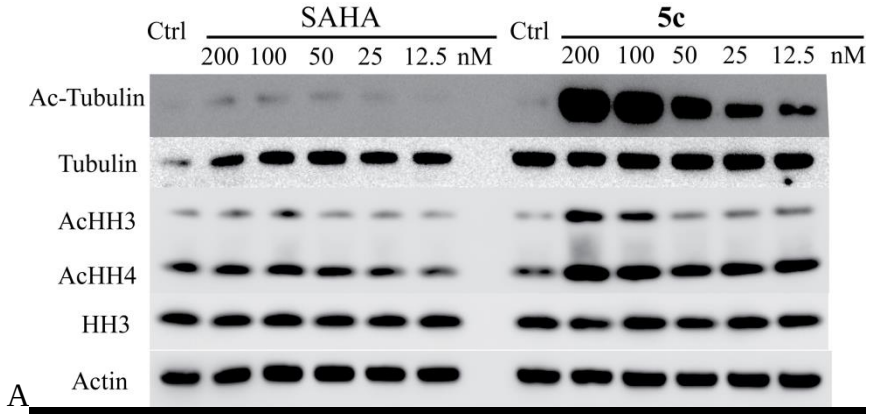

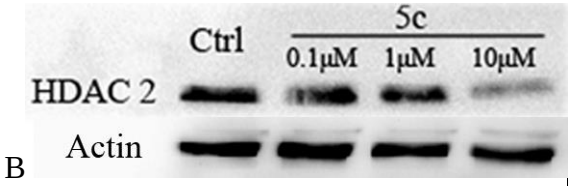

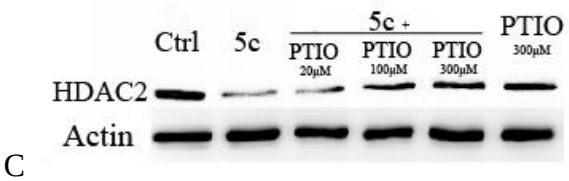

C

Sheme 1. The synthesis of compounds **5a-5o**

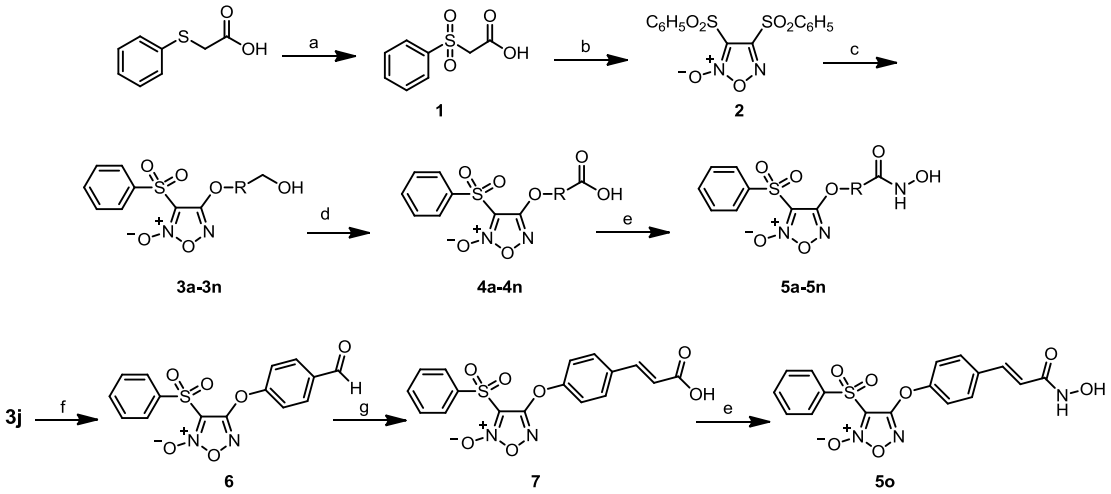

3a, 4a, 5a: R=$(CH_2)_3$
3b, 4b, 5b: R=$(CH_2)_4$
3c, 4c, 5c: R=$(CH_2)_5$
3d, 4d, 5d: R=$(CH_2)_6$
3e, 4e, 5e: R=$(CH_2)_7$
3f, 4f, 5f: R=$(CH_2)_2O\ CH_2$
3g, 4g, 5g: R=$CH_2C(CH_3)_2$
3h, 4h, 5h: R=CH_2CHCH
3i, 4i, 5i: R=$(CH_2CH_2O)_2CH_2$
3j, 4j, 5j: R=p-Ph
3k, 4k, 5k: R=m-Ph
3l, 4l, 5l: R=p-2-(CH_3O)-Ph
3m, 4m, 5m: R=p-Ph-CH_2
3n, 4n, 5n: R=$CH_2C(CH_3)(CH_2CH_2CH_3)$

Reagents and conditions: a) H_2O_2, CH_3COOH; b) conc.HNO_3; c) linker with two hydroxyl groups, 25%NaOH; d) *Jones* agent, acetone; e) Isobutyl chlorocarbonate, TEA, THF; $NH_2OH.HCl$, CH_3OH. f) PCC, DCM, 0℃;g) propandioic acid, Pyrrolidine, Py, reflux.

Table of Contents graphic: